

ตัวแบบเชิงคำนวณของภาวะพลาสติกของไซแนปส์ในบริเวณ CA1  
ของสมองส่วนฮิปโปแคมปัส

นายธีระพล สลีวงศ์

วิทยานิพนธ์นี้เป็นส่วนหนึ่งของการศึกษาตามหลักสูตรปริญญาวิทยาศาสตรดุษฎีบัณฑิต  
สาขาวิชาวิศวกรรมชีวเวช (สหสาขาวิชา)  
คณะวิศวกรรมศาสตร์ จุฬาลงกรณ์มหาวิทยาลัย  
ปีการศึกษา 2554  
ลิขสิทธิ์ของจุฬาลงกรณ์มหาวิทยาลัย

บทคัดย่อและแฟ้มข้อมูลฉบับเต็มของวิทยานิพนธ์ตั้งแต่ปีการศึกษา 2554 ที่ให้บริการในคลังปัญญาจุฬาฯ (CUIR)  
เป็นแฟ้มข้อมูลของนิสิตเจ้าของวิทยานิพนธ์ที่ส่งผ่านทางบัณฑิตวิทยาลัย

The abstract and full text of theses from the academic year 2011 in Chulalongkorn University Intellectual Repository (CUIR)  
are the thesis authors' files submitted through the Graduate School.

THE COMPUTATIONAL MODEL OF SYNAPTIC PLASTICITY  
IN AREA CA1 OF HIPPOCAMPUS

Mr. Teerapol Saleewong

A Dissertation Submitted in Partial Fulfillment of the Requirements for  
the Degree of Doctor of Philosophy Program in Biomedical Engineering

(Interdisciplinary Program)

Faculty of Engineering

Chulalongkorn University

Academic Year 2011

Copyright of Chulalongkorn University

Thesis Title	The Computational Model of Synaptic Plasticity in area CA1 of Hippocampus
By	Mr. Teerapol Saleewong
Field of Study	Biomedical Engineering
Thesis Advisor	Professor Anan Srikiatkachorn, M.D.
Thesis Co-advisor	Assistant Professor Anusorn Chonwerayuth, Ph.D.

---

Accepted by the Faculty of Engineering, Chulalongkorn University in Partial Fulfillment of the Requirements for the Doctoral Degree

..... Dean of the Faculty of Engineering  
(Associate Professor Boonsom Lerdhirunwong, Dr.Ing.)

THESIS COMMITTEE

..... Chairman  
(Associate Professor Watcharapong Khovidhungij, Ph.D.)

..... Thesis Advisor  
(Professor Anan Srikiatkachorn, M.D.)

..... Thesis Co-advisor  
(Assistant Professor Anusorn Chonwerayuth, Ph.D.)

..... Examiner  
(Assistant Professor Saknan Bongsebandhu-phubhakdi, Ph.D.)

..... External Examiner  
(Associate Professor Usa Humphries, Ph.D.)

ธีระพล สติวงศ์: ตัวแบบเชิงคำนวณของภาวะพลาสติกของไซแนปส์ในบริเวณ CA1 ของสมองส่วนฮิปโปแคมปัส (The Computational Model of Synaptic Plasticity in area CA1 of Hippocampus) อ.ที่ปรึกษาวิทยานิพนธ์หลัก: ศ.นพ.อนันต์ ศรีเกียรติขจร, อ.ที่ปรึกษาวิทยานิพนธ์ร่วม: ผศ.ดร.อนุสรณ์ ชนวีระยุทธ, 64 หน้า

การเกิดศักย์ระยะยาว (LTP) เป็นรูปแบบในการเพิ่มสมรรถนะในการปรับเปลี่ยนของสภาพประสาทประสาท และยอมรับโดยทั่วไปว่าเป็นตัวแบบของการเรียนรู้และจดจำ การเปลี่ยนแปลงระยะยาวนี้มีความซับซ้อนและเกี่ยวข้องกับหลายกระบวนการในจุดประสานประสาท ในงานวิจัยนี้อาศัยวิธีการตัดชิ้นเนื้อสมองแบบนอกร่าง (in vitro) เพื่อศึกษาประสิทธิภาพการกระตุ้นแบบความถี่สูงเพียงชั่วขณะ และแบบช่วงที่ต่ำ (TBS) ในการเหนี่ยวนำให้เกิด LTP ในหนูทดลอง นอกจากนี้ได้ศึกษาถึงผลของการลดขนาดและแผ่ขยายของคลื่นสมองของผิวสมองใหญ่ (CSD), picrotoxin-สารยับยั้งตัวรับ GABA<sub>A</sub> ต่อการเหนี่ยวนำ LTP ด้วยความถี่สูงเพียงชั่วขณะ เมื่อพิจารณาประสิทธิภาพของรูปแบบการกระตุ้น พบว่าการกระตุ้นด้วยความถี่สูงเพียงชั่วขณะใช้ความแรง  $0.37 \pm 0.0677V$  ในขณะที่กระตุ้นแบบ TBS ใช้  $0.31 \pm 0.0862V$  ซึ่งไม่พบความแตกต่างแบบมีนัยสำคัญจากทั้งสองกลุ่ม (one-way ANOVA,  $P=0.122$ ) สำหรับการเกิด LTP พบว่าการกระตุ้นแบบ TBS มีประสิทธิภาพเหนี่ยวนำให้เกิด LTP ได้สูงกว่าการกระตุ้นด้วยความถี่สูงเพียงชั่วขณะ โดยได้ LTP,  $144.42 \pm 6.54\%$  ( $N=10$ ) และ  $134.88 \pm 6.92\%$  ( $N=10$ ) ตามลำดับเมื่อเทียบกับค่าเริ่มต้น นอกจากนี้พบว่ากลุ่ม picrotoxin ได้ผลการเหนี่ยวนำ LTP สูงกว่ากลุ่มควบคุม โดยได้ LTP  $140.25 \pm 4.18\%$  ( $N=8$ ) และ  $134.88 \pm 6.92\%$  ( $N=10$ ) ตามลำดับเมื่อเทียบกับค่าเริ่มต้น สำหรับกลุ่ม picrotoxin ร่วมกับ CSD ได้ค่า LTP น้อยที่สุด ( $120.15 \pm 3.73\%$  เมื่อเทียบกับค่าเริ่มต้น,  $N=8$ ) จากข้อมูลการทดลอง นำมาปรับเส้นโค้งด้วยวิธีกำลังสองน้อยที่สุด ด้วยตัวแบบสมการเชิงคณิตศาสตร์ประกอบด้วยสมการเชิงพหุนาม สมการเชิงเลขชี้กำลัง และสมการเชิงเลขยกกำลัง พบว่าตัวแบบเชิงเลขยกกำลังได้ค่า adjusted  $R^2$  สูงสุดและสามารถประมาณค่าตั้งต้นของ ศักย์หลังการกระตุ้นชั่วขณะได้ดีที่สุด สำหรับการประมาณค่า LTP ทำให้ใกล้เคียงกันในสามตัวแบบ โดยตัวแบบเชิงพหุนาม ให้ความคลาดเคลื่อนสัมพัทธ์ของการประมาณ LTP น้อยแต่พบส่วนตกค้างจากการปรับข้อมูลสูง ในขณะที่ตัวแบบเชิงเลขยกกำลังและตัวแบบเชิงเลขชี้กำลังพบส่วนตกค้างจากการปรับข้อมูลน้อยกว่า ดังนั้นเมื่อเปรียบเทียบโดยภาพรวมแล้ว ตัวแบบเชิงเลขยกกำลังมีความเหมาะสมที่สุดในการประมาณค่า LTP หรือในการอธิบายผลจากการกระตุ้นในจุดประสานประสาทอื่นๆ นอกจากนี้คุณลักษณะไม่เชิงเส้นของ LTP ยังมีผลต่อการปรับข้อมูลในการเพิ่มความเที่ยงตรงของพารามิเตอร์ และเป็นคุณลักษณะหนึ่งในองค์ประกอบของการกระตุ้นให้เกิด LTP

สาขาวิชา วิศวกรรมชีวเวช .....ลายมือชื่อ.....

ปีการศึกษา 2554 .....ลายมือชื่อ อ.ที่ปรึกษาวิทยานิพนธ์หลัก.....

ลายมือชื่อ อ.ที่ปรึกษาวิทยานิพนธ์ร่วม.....

# # 4989741021: MAJOR BIOMEDICAL ENGINEERING

KEYWORDS: LONG-TERM POTENTIATION (LTP), HIPPOCAMPUS, CORTICAL SPREADING DEPRESSION (CSD), GAMMA-AMINOBUTYRIC ACID A (GABA<sub>A</sub>) RECEPTOR, TETANIC STIMULATION, THETA-BURST STIMULATION, LEAST SQUARES CURVE FITTING

TEERAPOL SALEEWONG : THE COMPUTATIONAL MODEL OF SYNAPTIC PLASTICITY IN AREA CA1 OF HIPPOCAMPUS., ADVISOR: PROF. ANAN SRIKIATKHACHORN, M.D., CO-ADVISOR: ASST. PROF. ANUSORN CHONWERAYUTH, Ph.D., 64 pp.

Long-term Potentiation (LTP) is the best characterized forms of enhancement in synaptic plasticity which is a widely accepted model of learning and memory. The modification of long-term plasticity is a complex process and varies throughout synaptic events. The present research, *in vitro* brain slice techniques were used to study the efficacy of tetanic stimulation and theta-burst stimulation (TBS) for LTP induction in rats. In addition, the study also investigated the effects of cortical spreading depression (CSD), picrotoxin-an antagonist of gamma aminobutyric acid A (GABA<sub>A</sub>) receptor on the tetanic-induced LTP.

For results of efficacy of stimulate patterns, the stimulation intensity was  $0.37 \pm 0.0677V$  with tetanic stimulation and  $0.31 \pm 0.0862V$  with TBS. There were no significant differences among groups (one-way ANOVA,  $P=0.122$ ). TBS effectively induces LTP more than tetanic stimulation with  $144.42 \pm 6.54\%$  of baseline (N=10) and  $134.88 \pm 6.92\%$  of baseline (N=10), respectively. In addition, the picrotoxin effectively induced LTP with  $140.25 \pm 4.18\%$  of the baseline in the picrotoxin group (N=8) versus  $134.88 \pm 6.92\%$  of the baseline in the control group (N=10). In group with picrotoxin applied to CSD, we obtained the smallest magnitude of LTP ( $120.15 \pm 3.73\%$  of the baseline, N=8).

The experimental data were interpreted by least squares curve fitting which modeled as three mathematical equations, polynomial, exponential and power equations. I found that the model of power equation produced the best in adjusted  $R^2$  value and initial post-tetanic potentiation approximation. For LTP approximation, there were similar quantification that the polynomial model produced a small relative error with abundant residual while there were not many residual from the exponential model and power model. Therefore, the power equation was a suitable model for LTP approximation or description of synaptic response. More over the nonlinear attribute of LTP had an influence on the fitting, with respect to increasing the accuracy of the parameters and the compatibility of combination of stimuli that produce LTP.

Field of Study: Biomedical Engineering, Student's Signature.....

Academic Year: 2011..... Advisor's Signature.....

Co-advisor's Signature.....

## ACKNOWLEDGEMENTS

I would like to express my sincere gratitude to my advisor, Professor Anan Srikiatkachorn and my co-advisor, Assistant Professor Anusorn Chonwerayuth for their excellent instruction, guidance, encouragement, and constructive criticism which enable me to carry out my study successfully. Grateful acknowledgement is also expressed to Assistant Professor Saknan Bongsebandhu-phubhakdi, who gave good advice and be guidance of this thesis since start until successful. He gave appreciate suggestion, checked and corrected the fault of this thesis and my manuscripts.

This thesis could not successfully complete without the kindness of Associate Professor Mana Sriyudthsak for the excellent instruction, for all comments and good suggestions.

I would like to thank Mr. Montree Maneepark who is a good guidance for experiment. I am also thankful to my family, my friends, all of biomedical engineering and neuroscience students for their loves and supports during this educational experience.

Finally my grateful is extended to Faculty of Science, King Mongkut's university of technology Thonburi for tuition fees supported and allowed me to undertake the Ph.D. program at Chulalongkorn University.

This study was supported by the Neuroscience of Headache Research Unit, the Thailand Research Fund (RTA5180004 and MRG5280061), Chulalongkorn Senior Scholar, and Ratchadaphiseksomphot Fund, Chulalongkorn University.

## CONTENTS

	<b>Page</b>
ABRTRACT (THAI).....	iv
ABRTRACT (ENGLISH).....	v
ACKNOWLEDGEMENTS.....	vi
CONTENTS.....	vii
LIST OF TABLES.....	ix
LIST OF FIGURES.....	x
LIST OF ABBREVIATIONS.....	xiii
CHAPTER I INTRODUCTION.....	1
CHAPTER II THEORY AND LITERATURE REVIEW.....	4
Synaptic function.....	4
The Hippocampus.....	6
Glutamatergic synaptic transmission.....	7
Gabaergic synaptic transmission.....	8
Long-term potentiation.....	9
Tetanic stimulation and theta-burst stimulation.....	11
Cortical spreading depression.....	12
Nonlinear least squares curve fitting.....	13
CHAPTER III MATERIALS AND METHODS.....	15
Animal preparation.....	15
Experimental protocols.....	15
Surgical procedures and induction of CSD.....	17
Preparation and maintenance of brain slices.....	18
Electrical stimulation and recording.....	19
Data acquisition and analysis.....	20
Least square curve fitting.....	21
CHAPTER IV RESULTS.....	23
Results from the experiments.....	23
Results from least squares curve fitting.....	30
CHAPTER V DISCUSSIONS AND CONCLUSIONS.....	41
The efficacy of nonlinear least square curve fitting.....	41

**CONTENTS**

	<b>Page</b>
CHAPTER V	
Computational approach for LTP describes their efficacy of stimulate patterns.....	42
Computational approach of altered LTP that used to investigated the effects of CSD and Picrotoxin on the synaptic plasticity.....	44
Conclusions.....	47
REFERENCES.....	48
APPENDICES.....	54
Appendix A.....	55
Appendix B.....	61
BIOGRAPHY.....	64



## LIST OF TABLES

	<b>Page</b>
Table 1 The parameters values of least square fitting, with data of stimulated patterns.....	33
Table 2 The parameters values of least square fitting, with control, Picrotoxin and Picrotoxin+CSD data.....	33
Table 3 Representative of first PTP of stimulated pattern experiments, comparison between experimental data and computational value; and $R_{adj}^2$ values.....	34
Table 4 Representative LTP of stimulated pattern experiments, comparison between experimental LTP and computational LTP.....	34
Table 5 Representative of first PTP of control, Picrotoxin and Picrotoxin+CSD groups, comparison between experimental data and computational value; and $R_{adj}^2$ values.....	35
Table 6 Representative LTP of control, Picrotoxin and Picrotoxin+CSD groups, comparison between experimental LTP and computational LTP.....	35

## LIST OF FIGURES

	<b>Page</b>
Figure 2.1 The synapse.....	5
Figure 2.2 Anatomy of the (rodent) Hippocampus.....	7
Figure 2.3 The coexistence of NMDA and AMPA receptors.....	8
Figure 2.4 Routes for the expression of LTP in CA1.....	10
Figure 3.1 (a) Diagram of experimental design for experiment of the patterns of Stimulation.....	17
Figure 3.1 (b) Diagram of experimental design for experiment of the effect of CSD and Picrotoxin.....	18
Figure 3.2 Induction of CSD in the brain of a Wistar rat.....	18
Figure 3.3 The electrode placement for LTP induction in area CA1 of the Hippocampus.....	19
Figure 3.4 Theta-burst stimulation is typically consisting of three trains of 10 brief 100 Hz burst, 4 impulses each, 200 msec between burst and repeated in 10seconds between train.....	20
Figure 3.5 The main window of HEKA software.....	20
Figure 3.6 An example of the raw fEPSPs, and the slope between the arrowheads is used for measuring fEPSP changes before and after tetanic stimulation/TBS as the LTP magnitude.....	21
Figure 4.1 The fEPSPs slope results from tetanic stimulation and theta-burst stimulation.....	24
Figure4.2 PTP in first 5 minutes after tetanic stimulation and theta-burst stimulation, each point plots 10 seconds time interval.....	25
Figure 4.3 A raw data of fEPSPs slope with n=10 which measured across the first 30 seconds after tetanic stimulation and theta-burst stimulation.....	25
Figure 4.4 Summary of fEPSPs slope of tetanic stimulation and theta-burst stimulation. The fEPSPs slope in recording period (60 min), <i>I</i> and <i>L</i> are representd initial and long term response respectively.....	26
Figure 4.5 Results of long term potentiations at the final 10 minutes of recording (50-60 min), each point plots the average of fEPSPs slop at interval 1 minute.....	26

## LIST OF FIGURES

	<b>Page</b>
Figure 4.6 The LTPs were induced under three different conditions. After 30 minutes with a stable baseline period (time -30 to 0), tetanic stimulation was applied at the 0 time point, and the post tetanic responses were continuously recorded for 60 min.....	27
Figure 4.7 The LTPs were induced under three different conditions. The measurements of the fEPSP slopes were plotted, for which each point was an average over every 6 values of 0.1 Hz (6 points in 1 minute).....	28
Figure 4.8 fEPSPs slope in the first 20 minutes after the tetanic stimulation.....	28
Figure 4.9 Results of LTPs at the final 10 minutes of recording (50-60 min).....	29
Figure 4.10 The experimental data of four different conditions. For the analysis, the error bar were removed.....	29
Figure 4.11 The LTPs were induced under four different conditions.....	30
Figure 4.12 The General plot of the data set in arbitrary units.....	31
Figure 4.13 The experimental results of the fEPSPs slope (% baseline) from tetanic stimulation. The lines represent curve fitted with least squares procedure, the insets show residual or error from curve fitting and the exact data. (a) Curve fitting with polynomial model, (b) Curve fitting with exponential model, (c) Curve fitting with power model.....	36
Figure 4.14 The experimental results of the fEPSPs slope (% baseline) from TBS. The lines represent curve fitted with least squares procedure, the insets show residual or error from curve fitting and the exact data. (a) Curve fitting with polynomial model, (b) Curve fitting with exponential model, (c) Curve fitting with power model.....	37
Figure 4.15 The experimental results of the fEPSP slopes (% baseline) from the control group. The lines represent the results of curve fitting with the nonlinear least squares procedure, the above inset show residuals from fitting. (a) Curve fitting with polynomial model, (b) Curve fitting with exponential model, (c) Curve fitting with power model.....	39

## LIST OF FIGURES

	<b>Page</b>
<p>Figure 4.16 The experimental results of the fEPSP slopes (% baseline) from the picrotoxin group. The lines represent the results of curve fitting with the nonlinear least squares procedure, the above inset show residuals from fitting.</p> <p>(a) Curve fitting with polynomial model, (b) Curve fitting with exponential (b) model, (c) Curve fitting with power model.....</p>	40
<p>Figure 4.17 The experimental results of the fEPSP slopes (% baseline) from the picrotoxin+CSD group. The lines represent the results of curve fitting with the nonlinear least squares procedure, the above inset show residuals from fitting. (a) Curve fitting with polynomial model, (b) Curve fitting with exponential model, (c) Curve fitting with power model.....</p>	40
<p>Figure 5.1 Rate of decay of PTP or the slope from the Eq. (4.2); parameter values in table 2 were used.....</p>	42

**LIST OF ABBREVIATIONS**

ACSF	Artificial cerebrospinal fluid
AMPA	$\alpha$ -amino-3-hydroxy-5-methyl-4-isoxazole propionate
CA	Cornu Ammonis,
CSD	Cortical spreading depression
EPSP	Excitatory post synaptic potential
fEPSP	Field excitatory post synaptic potential
GABA	Gamma-aminobutyric acid
HFS	High frequency stimulation
IPSP	Inhibitory postsynaptic potential
LTP	Long-term potentiation
NMDA	<i>N</i> -methyl-D-aspartate
PKA	Protein kinase A
PTP	Post-tetanic potentiation
TBS	Theta-burst stimulation

# CHAPTER I

## INTRODUCTION

### Background and Rationale

Long-term potentiation (LTP) is an enhancement of synaptic strength or synaptic plasticity that can persist for hours and perhaps even for a lifetime (Bliss and Collingridge 1993; Connor, 2009: 323-350). Hippocampal LTP is a widely accepted model of learning and memory (Bliss and Collingridge, 1993; Crozier et al., 2004: 109-122; Morgan and Teyley, 2001). The induction of LTP is usually achieved with high frequency stimulation (HFS) (Crozier et al., 2004; Hernandez et al., 2005; Manninen et al., 2010). Tetanic stimulation or tetanus stimulation is a brief burst of HFS (100 Hz for 1 second) of an excitatory pathway that can also produce the LTP in the hippocampus. When the synaptic potentiation decays after tetanic stimulation, it is called post-tetanic potentiation (PTP), which occurs within 10 minutes (Zucker, 1989; Tang and Zucker, 1997; Lee et al., 2010).

However, HFS is different patterns from naturally occurring firing patterns of neurons (Albeni et al., 2007) and tetanus do not correspond the innate activity in the intact animal during learning behaviorally (Morgan and Teyley, 2001). In response to these criticism, theta-burst stimulation (TBS) were developed that highly effective and perhaps optimal for induction of LTP (Larson and Lynch, 1986). TBS patterned mimics endogenous theta rhythms in the hippocampus that occur during some forms of learning and exploratory behavior (Crozier et al., 2004). Therefore tetanus and TBS are effective increasing synaptic transmission, there are different from efficiencies and physiological relevance.

One aspect of hippocampus studies is cortical spreading depression (CSD) which is a propagating wave of cellular depolarization that is believed to be a suppositional neuronal mechanism underlying migraine aura and pain (Leao and Morrison, 1945; Dehbandi et al., 2008; Edelstein and Mauskop, 2009; Rogawski, 2012). Because information on the effects of CSD on hippocampal activity has not been fully investigated, the effects of CSD on LTP induction in hippocampal tissue could yield confounding results. However, experimental investigations have indicated that disturbances in hippocampal synaptic transmission can be triggered by the propagation of CSD (Wernsmann et al., 2006).

Another influence on the incidence of LTP is the presence of a GABAergic interneuron. GABA receptors are a class of receptors that respond to the neurotransmitter

GABA, the principal inhibitory neurotransmitter in the vertebrate central nervous system. There are two main classes of GABA receptors, the GABA<sub>A</sub> and the GABA<sub>B</sub> type. When activated, the GABA<sub>A</sub> receptor conducts Cl<sup>-</sup> influx through its pore, resulting in hyperpolarization of the neuron. This scenario causes an inhibitory effect on the neurotransmission by reducing the chance of a successful action potential occurring. Moreover, a well-known noncompetitive antagonist for the GABA<sub>A</sub> receptor is picrotoxin.

Hippocampal LTP has been studied as a model of learning and memory (Bliss and Collingridge, 1993; Crozier et al., 2004). The hippocampus contains a population of neurons with powerfully nonlinear properties (Berger et al., 1994). In addition, synaptic transmission is a nonlinear dynamic process that plays a critical characterization role in signal transmission and information processing in the nervous system (Song et al., 2009). Recently, many computational models have been developed to investigate which interactions are critical for synaptic plasticity (Manninen et al., 2010; Kitajima et al., 2002; Migliore and Lansky, 1999; Miglior et al., 1995). One of the techniques for improving these models is to fit experimental data (Holmes et al., 2006; Holmes and Grover, 2006; Nieuwenhuis et al., 2006).

As mentioned above, there are many factors, such as the pattern of stimuli, the capabilities of receptors and CSD occurrences, that could alter synaptic plasticity and effectiveness. In this research, I investigated LTP under conditions with a GABA<sub>A</sub> receptor antagonist and CSD. I therefore investigated whether a comparison of tetanic stimulation and TBS would produce difference in magnitude of LTP in area CA1 of the hippocampus. Furthermore, LTP has been analyzed with least squares curve fitting to predict the magnitude of the LTP and to approach characterizing the response of the hippocampal neurons.

### **Research Questions**

1. How does synaptic plasticity differ when observed at different conditions (patterns of stimuli, GABA<sub>A</sub> receptor antagonist and CSD)? Do these conditions effect to the LTP magnitude?
2. What are the quantitative representation of altered LTP in the CA1 hippocampal synapse, i.e., the LTP described by mathematical or computational models?

### **Research Objectives**

1. To study the synaptic plasticity and LTP under conditions with the patterns of stimuli, the GABA<sub>A</sub> receptor antagonist and CSD.

2. To quantify the altered LTP in the CA1 hippocampal synapse.

### **Hypothesis**

The altered LTP are quantified by least squares curve fitting and nonlinear attribute of LTP has an influence on the fitting.

### **Expected Benefit and Application**

Experimental data would give an understanding of the altered LTP and synaptic plasticity at different conditions. The computational approach for LTP could be developed to reasonably model and can help to validate mechanisms in neurophysiology processes.



## **CHAPTER II**

### **THEORY AND LITERATURE REVIEW**

The nerve system is unique in the complication of thought process and control achievements it can perform. The brain is a network of more than one hundred billion individual neurons interconnected in systems, and the point at which one neuron communicates with another is called synapse. Although many of these communications are highly specialized, all neurons apply one of the two general types of synaptic transmission, electrical or chemical. Besides, the strength of both types of synaptic transmission can be increased or reduced by cellular activity. This plasticity in nerve cells is very important to learning and other higher brain functions which is especial implication in this thesis. Moreover, I explain the theory of nonlinear least squares curve fitting that will be used to improve the efficacy of computational models.

#### **Synaptic Function**

##### **1. Synaptic Transmission**

A synapse is the specialized connection where one part of a neuron contacts with and transfers information to another neuron or cell type (such as a muscle). The synapse has two sides, indicating that the information tends to flow in one direction, from a neuron to its target cell. The presynaptic side generally consists of an axon terminal, while the postsynaptic side may be the dendrite or soma of another neuron (Figure 2.1). The space between the presynaptic and postsynaptic membranes is called the synaptic cleft. The transfer of information at the synaptic from one neuron to another is called synaptic transmission, which divided into two different types of synapse. Electrical synapses are relatively simple in structure and function, and they allow the direct transfer of ionic current from one cell to the next (Bear, Connors and Paradiso, 2007: 40,102-103). Most of these consist of small protein tubular structures called gap junctions that allow free movement of ions from the interior of one cell to the interior of the next (Guyton and Hall, 2006: 559).

Chemical synapse is a main characteristic of synaptic transmission in mature human nervous system, which requires the efficiency of neurotransmitters. The researchers have been identifying neurotransmitters in brain as three chemical categories: amino acids, amines and

peptides. Different neurons in the brain release different neurotransmitters. Fast synaptic transmission at most central nerve system synapses is mediated by the amino acids glutamate, gamma-aminobutyric acid (GABA), and glycine (Beer et al., 2007:111-112).

Neurotransmitter released into the synaptic cleft affects the postsynaptic neuron by binding to specific receptor proteins. A transient postsynaptic membrane depolarization caused by the presynaptic release of neurotransmitter is called an excitatory post synaptic potential (EPSP). Synaptic activation of glutamate-gated ion channels causes EPSP. On the contrary, inhibitory postsynaptic potential (IPSP) is transient hyperpolarization of the postsynaptic membrane potential caused by the presynaptic release of neurotransmitter. Synaptic activation of GABA-gated ion channels is one cause of IPSP (Beer et al., 2007:117).

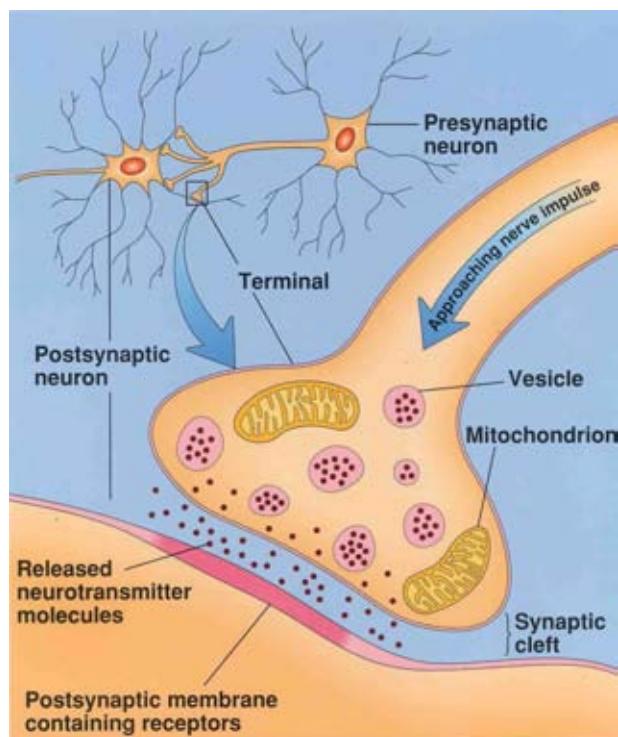


**Figure 2.1** The synapse (<http://www.unc.edu/~ejw/synapse.html>)

## 2. Synaptic plasticity

Synaptic plasticity is a process in which synapses change their efficacy as a result of their previous activity (Jedlicka, 2002: 138). It is widely believed that plastic changes in the strengths of synaptic connections between neurons are central to the process of information storage in the brain. Many forms of this type of change have been described from various regions of the central nervous system (Larkman, 1995). A synaptic efficacy may arise

from the presynaptic terminal releasing more or less neurotransmitter in response to an action potential, and the postsynaptic neuron has increased or reduced its response to the transmitter (Brodal, 2010: 50).

Several kinds of synaptic plasticity have been described on the basis of animal experiments, and more are probably yet to be discovered (Brodal, 2010: 50). It is usual to divide between short term and long term synaptic plasticity. Short term plasticity lasts less than 30 minutes and some forms only last for milliseconds to seconds, whereas long term plasticity normally lasts longer than 30 minutes (Huang, 2010: 14).

## **The Hippocampus**

The elementary properties of synaptic plasticity have been most extensively studied in the hippocampus, a structure critically involved in learning and memory (Squire, 1992). The hippocampus has a well-characterized laminar organization that is advantageous for electrophysiological stimulation. Because of this organization, electrophysiologists can stimulate a fairly homogeneous population of axons and record their monosynaptic responses (Crozier et al., 2004: 109).

The hippocampus consists of two thin sheets of neurons folded onto each other. One sheet is called the dentate gyrus, and the other sheet is called Ammon's horn. Of the four divisions of Ammon's horn, we will focus on two: CA3 and CA1 (CA stands for cornu Ammonis, Latin for "Ammon's horn") (Beer et al., 2007: 777).

The Hippocampus has three major pathways: (1) the perforant pathway, which projects from the entorhinal cortex to the granule cells of the dentate gyrus; (2) the mossy fiber pathway, which contains the axons of the granule cells and runs to the pyramidal cell in the CA3 region of the hippocampus and (3) the Schaffer collateral pathway, which consists of the excitatory collaterals of the pyramidal cells in the CA3 region and ends on the pyramidal cell in the CA1 region (Kandel, Schwartz, Jessell, 2000: 1259). These connections are summarized in Figure 2.2.

In the late 1960s, researchers discovered that the hippocampus actually could be removed from the brain (usually in experimental animals) and cut up like a loaf of bread, and that the resulting slices could be kept alive *in vitro* for many hours. Because cells in the slice can be positioned with the precision previously reserved for invertebrate preparations. In such a brain slice preparation, fiber tracts can be stimulated electrically and synaptic responses recorded. (Beer et al., 2007: 777-778). Although several forms of synaptic plasticity exist

throughout the brain, available data suggest that the Schaffer collateral-CA1 synapse is a reasonable model for many other cortical synapses (Crozier et al., 2004: 109). Therefore, synaptic plasticity in CA1 will be the focus of this thesis.

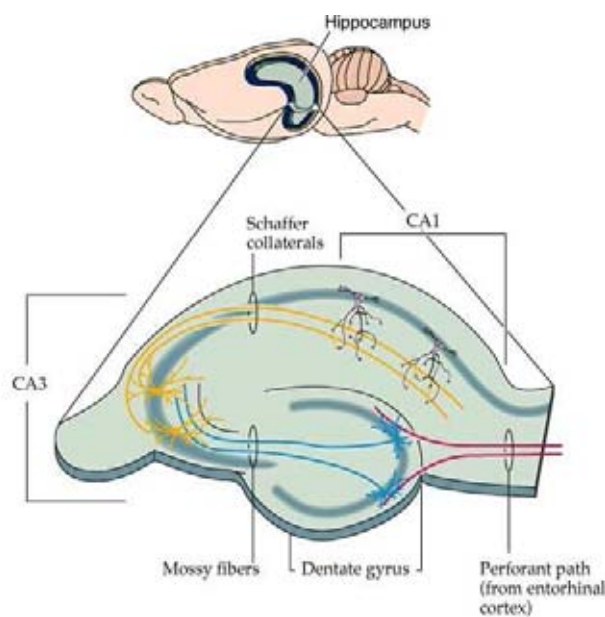


**Figure 2.2** Anatomy of the (rodent) Hippocampus.  
 (<http://www.arts.uwaterloo.ca/~bfleming/psych261/lec15no7.htm>)

## Glutamatergic Synaptic Transmission

The Hippocampal CA3-CA1 synapses have been used as a principle model system for learning the synaptic transmission and synaptic plasticity. These synapses are excited and utilize glutamate as neurotransmitter. Glutamate is secreted by the presynaptic terminals in many of the sensory pathways entering the central nervous systems, as well as in many areas of the cerebral cortex. It is believed to be the cause of excitation (Guyton and Hall, 2006: 564).

The glutamate receptors can be divided into two broad categories: the ionotropic receptors that directly gate channels and the metabotropic receptors that indirectly gate channels through second messengers. There are three major subtypes of ionotropic glutamate receptors:  $\alpha$ -amino-3-hydroxy-5-methyl-4-isoxazole propionate (AMPA) receptors, *N*-methyl-D-aspartate (NMDA) receptor and kainite receptors. Each named according to the types of synthetic agonists that activate them (Kandel et al., 2000: 212).

AMPA-gated channels are permeable to both  $\text{Na}^+$  and  $\text{K}^+$  and most of them are not permeable to  $\text{Ca}^{2+}$ . The net effect of activating them at normal, negative membrane potentials is to admit  $\text{Na}^+$  ions into the cell, causing a rapid and large depolarization. NMDA-gated channels also cause excitation of a cell by admitting  $\text{Na}^+$ , but they differ from AMPA receptors in two aspects: NMDA-gated channels are permeable to  $\text{Ca}^{2+}$ , and inward ionic current through NMDA-gated channels is voltage dependent (Bear et al., 2007: 154-155), see more detail in Figure 2.3. It is widely accepted that NMDA receptors are crucial for LTP development (Abarbanel, Huerta and Rabinovich, 2002: 10132).

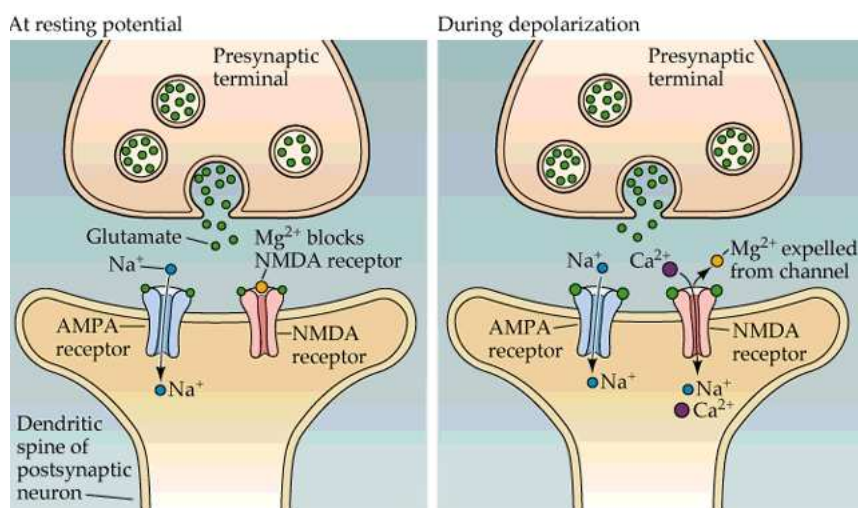
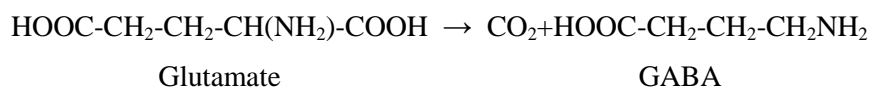


**Figure 2.3** The coexistence of NMDA and AMPA receptors

(<http://www.arts.uwaterloo.ca/~bfleming/psych261/lec15no7.htm>)

## GABAergic Synaptic Transmission

Gamma-aminobutyric acid (GABA) is neurotransmitter that GABAergic neurons are the major source of synaptic inhibition in the central nervous system. The GABA is synthesized from glutamate in a reaction catalyzed by glutamic acid decarboxylase (Kandel, 2000: 285), this reaction as:



The GABA acts on two receptors,  $\text{GABA}_A$  and  $\text{GABA}_B$ . The  $\text{GABA}_A$  receptor is an ionotropic receptor that gates a  $\text{Cl}^-$  channel. The  $\text{GABA}_B$  receptor is a metabotropic receptor

that activates a second-messenger cascade, which often activates a  $K^+$  channel (Kandel et al., 2000: 214).

The  $GABA_A$  receptor is a transmitter-gated chloride channel that requires five subunits for each channel and the  $GABA$ -gated channels are influential roles in disease and drugs achievement. Picrotoxin is one of the antagonist of  $GABA_A$  receptor. It blocks chloride ion flow through the channel. Picrotoxin is clearly a noncompetitive antagonist, acting not at the  $GABA$  recognition site but perhaps within the ion channel (Olsen, 2006: 6081).

## **Long-Term Potentiation**

Synaptic effectiveness can be altered in most nerve cells by intense activity. In these cells a high-frequency train of action potentials is followed by a period during which action potentials produce successively larger postsynaptic potentials. High-frequency stimulation of the presynaptic neuron is called tetanic stimulation. The increase in size of the postsynaptic potentials during tetanic stimulation is called potentiation; the increase that persists after tetanic stimulation is called posttetanic stimulation. This enhancement usually last several minutes, but it can persist for an hour or more (Kandel et al., 2000: 274)

In 1973, Timothy Bliss and Terje Lomo discovered that a brief high-frequency electrical stimulation to any of an excitatory pathway to the hippocampus produced a long-lasting enhancement in the strength of the stimulated synapses. This effect is now known as a long-term potentiation or LTP.

### **1. Properties of Long-term potentiation (LTP) in CA1.**

Although LTP was first demonstrated at the perforant path synapses on the neurons of the dentate gyrus, today most of the experiments on the mechanism of LTP are performed on the Schaffer collateral synapses on the CA1 pyramidal neurons in brain slice preparations.

In a typical experiment, the effectiveness of the Schaffer collateral synapse is monitored by giving a bundle of presynaptic axons a brief electrical stimulus and then measuring the size of the resulting EPSP in a postsynaptic CA1 neuron. This method is similar to the way parallel fiber responses are monitored in the cerebellar cortex. Usually, such a test stimulation is given every minute or so for 15-30 minutes to ensure that the baseline response is stable. Then, to induce LTP, the same axons are given a tetanic stimulation. Usually, this tetanic induces LTP, and subsequent test stimulation evokes an

EPSP that is much greater than it was during the initial baseline period (Beer et al., 2007: 778).

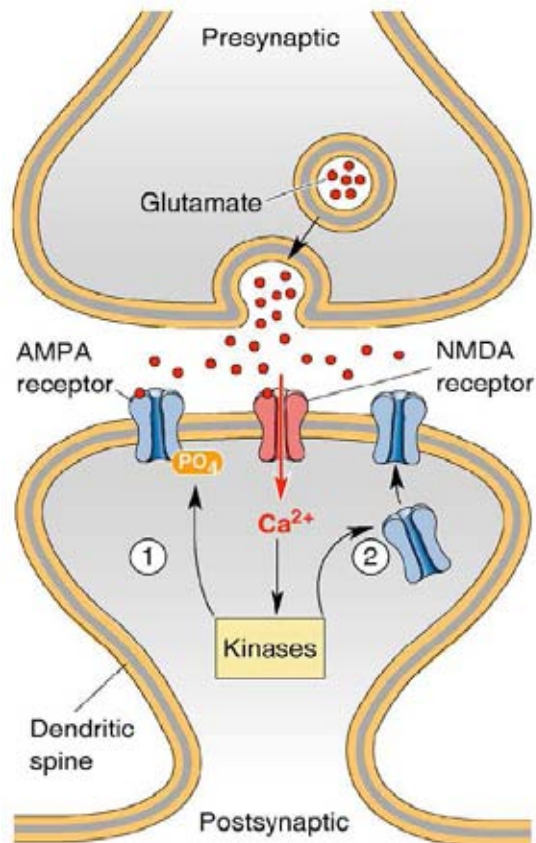


**Figure 2.4** Routes for the expression of LTP in CA1. Ca<sup>2+</sup> passing through the NMDA receptor activate protein kinases. This can cause LTP by (1) changing the effectiveness of existing postsynaptic AMPA receptors or (2) stimulating the insertion of new AMPA receptors (Bear et al., 2007: 781).

## 2. Mechanisms of LTP in CA1.

Excitatory synaptic transmission in the hippocampus is mediated by glutamate receptors. During normal, low-frequency synaptic transmission glutamate is released from the presynaptic terminal and acts both the NMDA and AMPA receptors. Na<sup>+</sup> and K<sup>+</sup> ions passing through the AMPA channels but not through the NMDA channels, owing to Mg<sup>2+</sup> blockage of this channel at the resting level of membrane potential. When the postsynaptic membrane is depolarized by the actions of the AMPA receptors-channels, as occurs during a high-frequency tetanic stimulation LTP, the depolarization relieves the Mg<sup>2+</sup> blockage of the NMDA channel. This allows Ca<sup>2+</sup> to flow through the NMDA channel (Kandel et al.,2000: 1260).

Considerable evidence now links this rise in postsynaptic  $\text{Ca}^{2+}$  concentration inside the cell,  $[\text{Ca}^{2+}]_i$  to the induction of LTP. The rise in  $[\text{Ca}^{2+}]_i$  activates two protein kinase: *protein kinase C* and *calcium-calmodulin-dependent protein kinase II*, also known as CaMKII. However, the molecular investigated that leads to a potentiated synapse gets difficultly to follow. Current research suggests that this investigated may actually two ways. One way appears to lead toward an increased effectiveness of existing postsynaptic AMPA receptors, by either protein kinase C or CaMKII, leads to a change in the protein that increase the ionic conductance of the channel. The orther way leaeds to the insertion of entirely new AMPA receptors into the postsynaptic membrane. According to a current model, vesicular organelles studded with AMPA receptors lie in wait near the postsynaptic membrane. In response to CaMKII activation, the vesicle membrane fuses with the postsynaptic membrane, and the new AMPA receptors are thereby delivered to the synapse. Evidence also indicates that synaptic structure changes following LTP.

### **Tetanic Stimulation and Theta-Burst Stimulation**

The induction of LTP is usually achieved with high frequency stimulation (HFS) (Crozier et al., 2004; Hernandez et al., 2005 and Manninen et al.,2010), which is a trains of 50-100 square pulses at 100 Hz (Bliss and Collingridge, 1993, Crozier et al., 2004, Hernandez et al., 2005, Manninen et al., 2010). Tetanic stimulation is a brief burst of HFS (100 Hz for 1 second) of an excitatory pathway that can also produce the LTP in the hippocampus (Beer et al., 2007). Moreover, Tetanic stimulation have been used and are effective for inducing both NMDA receptor-dependent and NMDA receptor independentforms of LTP (Albensi et al., 2007).

However, tetanic stimulation is different patterns from naturally occurring firing patterns of neurons. It is not reliable that hippocampal neurons in the alive animal fire at 100 Hz for one full second, making tetanic sitmulation questionable. CA1 hippocampal pyramidal cells usual fire for only 30–40 ms bursts of three to four spikes (Feder and Ranck, 1973; Kandel and Spencer, 1961; Kandel et al., 1961; Ranck, 1973).

In response to this evaluation, other stimulation protocols such as theta-burst stimulation (TBS) (Graves et al., 1990; Morgan and Teyler, 2001; Pavlides et al., 1988) was developed (explained below) and appears capable of LTP induction based on the physiology of hippocampus (Albensi et al., 2007). TBS patterned mimics endogenous theta rhythms in the hippocampus that occur during some forms of learning and exploratory behavior



(Crozier et al., 2004). The observation of the hippocampal electroencephalographic waveform in rats was shown to be dominated by a 5 to 12 Hz (theta,  $\theta$ ) frequency, observed when animals are occupied in learning-related exploratory behaviors (Grastyan et al., 1959). Furthermore, the theta-rhythm has been recorded in the CA1 subfield and the dentate gyrus of the hippocampus (Winson, 1972), and also in entorhinal cortex Ammon's horn, subiculum and cingulate gyrus (Furukawa et al., 1996).

Given that theta burst stimulation seemed effective for LTP induction, investigations were also conducted addressing whether or not theta burst stimulations were also effective for long-lasting LTP. To this end, Nguyen et al. (1994) studied theta burst stimulation (3 seconds of theta: 15 bursts of 4 pulses at 100 Hz; pulse width 50  $\mu$ s; interburst interval 200 ms) in CA1 mouse hippocampal slices and discovered that the LTP response was sustained out to 180 min post stimulation, whereas LTP induced by 60 Hz for 1 s had decayed back to near-baseline levels by this time point. However, Nguyen and Kandel did not observe and compare the usual 100 Hz HFS in this study.

Until currently, little was really understood about the mechanisms of theta burst. The recent data show that theta burst stimulation, like HFS, in area CA1 also implicates transcription, translation, and protein kinase A (PKA) activation (Nguyen et al., 1994).

### **Cortical Spreading Depression**

Cortical spreading depression (CSD) is a propagating of cellular depolarization which is a brief depolarization wave that slowly spreads across the cortex at a rate of 3-5 mm per minute (Lauritzen, 1994). The phenomenon of CSD was originally described by Aristides Leao, who was studying a model of experimental epilepsy. When electrical stimulation was applied to the cortical surface of rabbits, the weak electrical stimulation obtained a reduction in the spontaneous activity (depression of the electrocorticogram signal) at the stimulated area (Leao 1944, Somjen 2005). CSD is postulated as a neuronal mechanism for migraine aura and the cause of subsequent headache pain (Rogawski, 2012:932).

The characteristic and growth of sensory disturbances during migraine auras suggests that the underlying mechanism is a disturbance of the cerebral cortex, probably the CSD (Lauritzen 1994). The good CSD explanation for migraine aura as the complex visual experience (for example, fortification auras) may be the result of the initial wave of activation. As the wave propagates over the visual cortex, the aura moves gradually from the center of the visual field out to the periphery. Negative experiences such as scotomas may be

the result of the subsequent cortical depression, following behind the wave of activation (Borkum, 2007:104).

The precise mechanism for initiation and propagation of CSD are still not fully understood. Ionotropic glutamate receptor channels was believed to play a role in CSD. The depolarization of CSD is supposed to relieve the block of magnesium within NMDA receptors at resting potential, and therefore AMPA receptors quickly desensitize (Rogawski, 2012:932). Actually, it has been known that glutamate can trigger CSD from the work of van Harreveld and Fifkova in the 1970s (Van and Fifkova, 1973). The glutamate-induced CSD was inhibited in occurring the high magnesium ion concentration (10-15 mM) and this concentration of magnesium is sufficient to block NMDA receptors. However in migraine NMDA receptors are crucial trigger for CSD but the nature of the ionic conductance that leads to the massive but transitory neuronal depolarization in CSD is yet to be defined (Rogawski, 2012:939).

As memories in humans rely on the medial temporal lobe system (composing the hippocampus), it was proposed that interictal memory dysfunction in patients with migraine corresponds with the hippocampus involvement. Classical investigation of hippocampal spreading depression more often by implantation of KCl into hippocampus and induced the spreading depression directly in tissue. However, the information on the effects of CSD on hippocampal activities are not much available (Wernsmann et al., 2006: 1103).

## Nonlinear Least Squares Curve Fitting

A nonlinear least squares problem arises when a parameterized function is fit to real data points by minimizing the sum of squared error between the data points, when the function is not linear in its parameters. Given a nonlinear model  $y(x, a_0, a_1, \dots, a_m)$ , the parameters  $a_0, a_1, \dots, a_m$  are estimated in the model. Then, the objective function for the minimization problem is

$$f(a_0, a_1, \dots, a_m) = \sum_{i=1}^n (y_i - y(x_i, a_0, a_1, \dots, a_m))^2,$$

which depends on the  $(m+1)$  variables  $a_0, a_1, \dots, a_m$ , and  $x_i$  are known values from the data.

However, the objective function is

$$\text{minimize } f(a) = \sum_{i=1}^n f_i^2(a_0, a_1, \dots, a_m)$$

where  $f_i = (y_i - y(x_i, a_0, a_1, \dots, a_m)), i = 1, 2, \dots, n$ .

The objective function is defined in terms of the auxiliary function  $\{f_i\}$ . Let an equation of the derivative in a least squares problem be

$$\text{minimize}_a f(a) = \sum_{i=1}^n f_i^2(a) \equiv F(a)^T F(a)$$

where  $F$  is the vector-valued function  $F(a) = (f_1(a) \ f_2(a) \ \dots \ f_n(a))^T$ .

Using the chain rule for the derivative,

$$\nabla f(a) = \nabla F(a) F(a) \quad (2.1)$$

and

$$\nabla^2 f(a) = \nabla F(a) F(a)^T + \sum_{i=1}^n f_i(a) \nabla^2 f_i(a). \quad (2.2)$$

These are the formulas for the gradient and Hessian of  $f$  ( $\nabla^2 f(a)$ , which are also denoted by  $H(x)$ ). In many cases of interest, the Jacobian  $J(a_0, a_1, \dots, a_m)$  of the vector  $f(a_0, a_1, \dots, a_m)$  is relatively easy to compute, and thus,  $\nabla f(a) = J^T F$  is the same gradient of  $f$  in Eq. (2.1). The solution of the least squares problem was determined to be  $a_*$ , and we suppose that  $F(a_*) = 0$ . It would be correct to expect that  $F(a)$  is close to zero for  $a \approx a_*$ , which implies that

$$\nabla^2 f(a) = \nabla F(a) F(a)^T + \sum_{i=1}^n f_i(a) \nabla^2 f_i(a) \approx \nabla F(a) F(a)^T. \quad (2.3)$$

Thus, the special technique of a nonlinear least squares problem is that the Hessian of the objective function result is a simple computation.

The main methods for solving nonlinear least squares problems are the Gauss-Newton method and the Levenberg-Marquardt method (Leader, 2004). In summary, the Gauss-Newton method computes a probe by Newton's method for the minimization of  $H(z_k)(z_{k+1} - z_k) = -\nabla f(z_k)$ . However, it replaces the Hessian with an approximation from Eq. (2.3),

$$\nabla F(z_k) F(z_k)^T (z_{k+1} - z_k) = -\nabla F(z_k) F(z_k). \quad (2.4)$$

For another algorithm for solving nonlinear least squares problems, specifically the Levenberg-Marquardt method, see (Leader, 2004; Marquard, 1963). This method is a combination of the gradient descent method and the Gauss-Newton method, which uses the equation

$$\left[ \nabla F(z_k) \nabla F(z_k)^T + \lambda_k D_k^T D_k \right] (z_{k+1} - z_k) = -\nabla F(z_k) F(z_k). \quad (2.5)$$

where  $\lambda_k \geq 0$  and  $D_k$  is a diagonal matrix such that it is the identity matrix for all  $k$ .

## CHAPTER III

### Materials and Methods

This research design was animal experimental design to study the cortical spreading depression (CSD) occurrences, an antagonist of GABA<sub>A</sub> and electrical stimulate patterns on changes of LTP and synaptic plasticity in rats. *In vitro* hippocampal brain slice techniques were used to investigate these effects for LTP where characteristics of hippocampal LTP are described by least squares curve fitting. The experimental data were modeled as three mathematical equations. Curve fitting with least squares procedure and parameters solving were computed from Levenberg-Marquardt method, with OriginPro 8.5 software.

#### Animal Preparation

Male Wistar rats were purchased from the National Laboratory Animal Center, Mahidol University, Salaya, Nakorn Pathom. The rats were kept in a controlled temperature room at 25±1°C under standard conditions (12 hour light: dark) and had freely access to food and tap water. All rats were received well care in accordance with the Ethical Committee, Faculty of Medicine, Chulalongkorn University, Thailand (approval No. 20/54).

#### Experimental Protocols

The experimental studies were divided into 2 sections. First, I investigated whether a comparison of tetanic stimulation and theta-burst stimulation (TBS) would produce difference in magnitude of LTP. Second, I investigated LTP under conditions with a GABA receptor antagonist (Picrotoxin) and CSD with tetanic stimulation. Therefore the groups of experiment are shown follow.

##### 1. Experiment of the patterns of stimulation

Male Wistar rats (250-450 g.) were divided into 2 groups: The LTP induced by tetanic stimulation (tetanic stimulation group, N =10) and the LTP induced by TBS (theta-burst stimulation group, N =10). There were same conditions of brain slices preparation. The study design was summarized in the Figure 3.1(a).

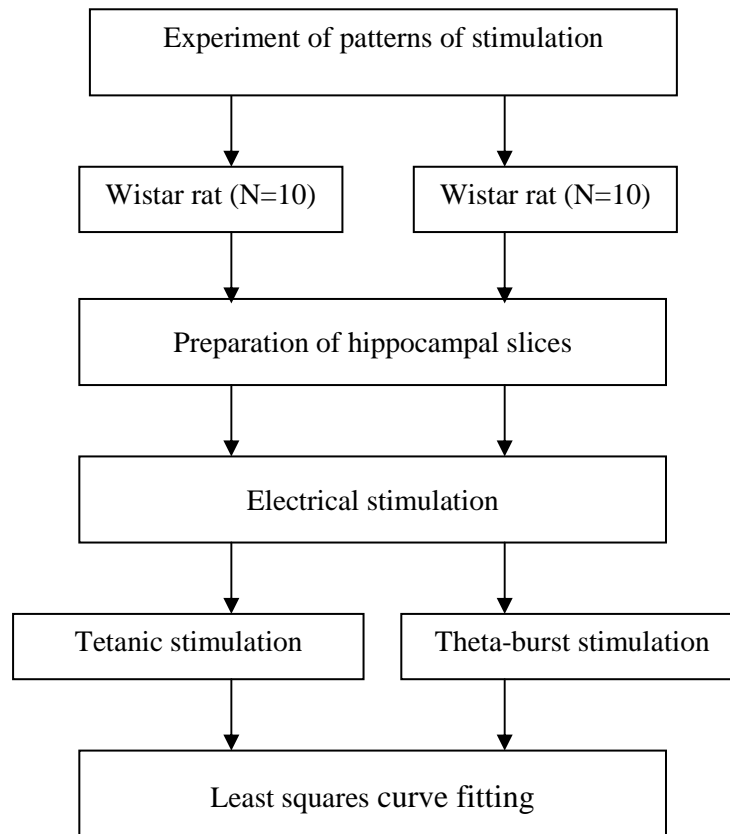


**Figure 3.1 (a)** Diagram of experimental design for experiment of the patterns of stimulation

## 2. Experiment of the effect of CSD and Picrotoxin

Male Wistar rats (250-450 g.) were divided into 3 groups: the LTP control (the control group, N=10), the LTP with picrotoxin (the picrotoxin group, N=8) and the LTP with picrotoxin and applied CSD (the picrotoxin+CSD group, N=8). The picrotoxin experiments were preparation and maintenance of brain slices in artificial cerebrospinal fluid (ACSF) with picrotoxin. On the other hand, the control group used ACSF without picrotoxin. The applied CSD was a procedure that done before the preparation of brain slices. All groups applied tetanic stimulation for LTP induction. The study design was summarized in the Figure 3.1(b).

However, tetanic stimulation from section 1 and the control group from section 2 were same conditions, thus there were collected as same data.

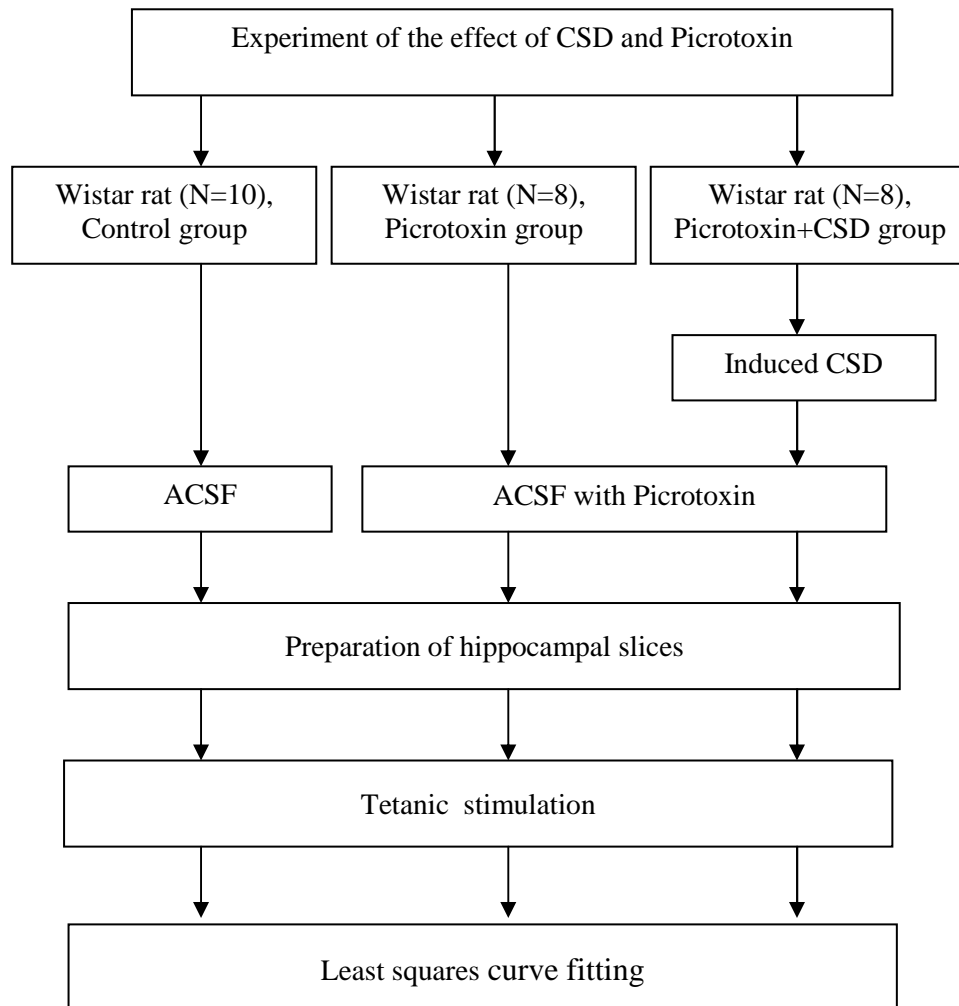


**Figure 3.1 (b)** Diagram of experimental design for experiment of the effect of CSD and Picrotoxin

### Surgical Procedures and Induction of CSD

The rats were anesthetized with sodium pentobarbital (60 mg/kg, intraperitoneally) and fitted with an intratracheal tube. Accessional doses of anesthetics were given as required to sustain surgical anesthesia based on the response to a tail pinch, to prevent the animal were feeling in pain during the experiment. Rats were placed in a stereotaxic apparatus. A midline surgical incision was executed, and the skin and soft tissue overlaying the skull were removed.

For the CSD induction process, a craniotomy that was 2 mm in diameter was performed on the right parietal bone (6 mm posterior to the bregma and 2 mm lateral to the midline). The bone was attentively drilled using a slow-speed, saline-cooled technique to minimize the surgical irritation of the neurons. Dura mater was uncovered by a micro needle.

Multiple waves of CSD were elicited by a topical application of solid KCl (3 mg) on exposed parietal cortex surface, as shown in Figure 3.2. Forty-five minutes later, the ipsilateral hippocampus was removed and was prepared for hippocampal slicing.

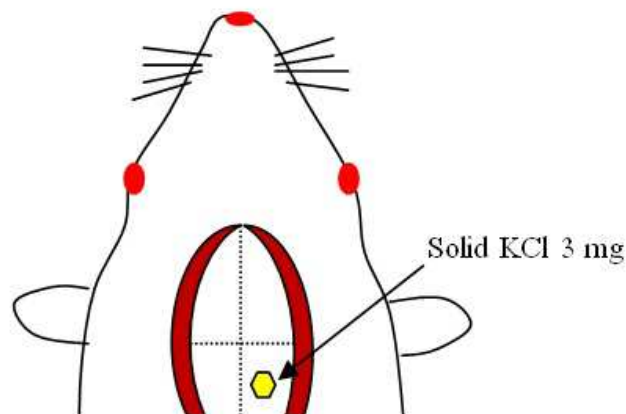


**Figure 3.2** Induction of CSD in the brain of a Wistar rat.

### **Preparation and Maintenance of Brain Slices**

Hippocampal slices were prepared from rats in all groups. The animals were decapitated after anesthesia (120 mg/kg of Thiopental Sodium, intraperitoneally injection). The brains was removed rapidly from skull and maintained in ice-cold ACSF consisted of the following: 119 mM NaCl, 2.5 mM KCl, 1.0 mM NaH<sub>2</sub>PO<sub>4</sub>, 26.2 mM NaHCO<sub>3</sub>, 11 mM glucose, 1.3 mM MgSO<sub>4</sub> and 2.5 mM CaCl<sub>2</sub>, oxygenated by 95% O<sub>2</sub> and 5% CO<sub>2</sub> (pH 7.3-7.4). The hippocampus of both sides was then dissected out from surrounding cortical tissue and sliced of 400 microns thickness, using a vibrating tissue slicer (Vibratome Instruments). The slices were maintained for 1-2 hours, stored in a holding chamber with oxygenation at temperature 22-24°C. For the electrophysiological experiments, slices were transferred to recording chambers and were immersed in ACSF at a rate of 2.3 ml/min with oxygenation and control as room temperature (22-24°C).

The LTP inductions were presented either in the presence or absence of the postsynaptic inhibition with the GABA antagonists. The picrotoxin had been used for this GABA<sub>A</sub> receptor blockage. I applied 0.1 mM picrotoxin in ACSF that used it in the picrotoxin group and the picrotoxin+CSD group.

## Electrical Stimulation and Recording

Stimulating and recording electrodes were positioned via micromanipulators in the slice under visual guidance under a microscope. Bipolar tungsten stimulating electrodes were placed into the Schaffer collateral in area CA1 (150 microns in deep). For extracellular recording of a neurons population or field excitatory postsynaptic potentials (fEPSPs) recording, a glass micropipette filled with 4 M NaCl (2-6 M $\Omega$  resistance) was used in the stratum radiatum of the CA1 area. The stimulus intensity was adjusted so that fEPSPs of 0.10-0.15 mV/ms slope. The fEPSP were elicited by adjusting the stimulation intensity ranging from 0.18V up to the intensity that yielded fEPSP of maximal slope. The position of the stimulating electrode and the recording electrode are shown in Figure 3.3.

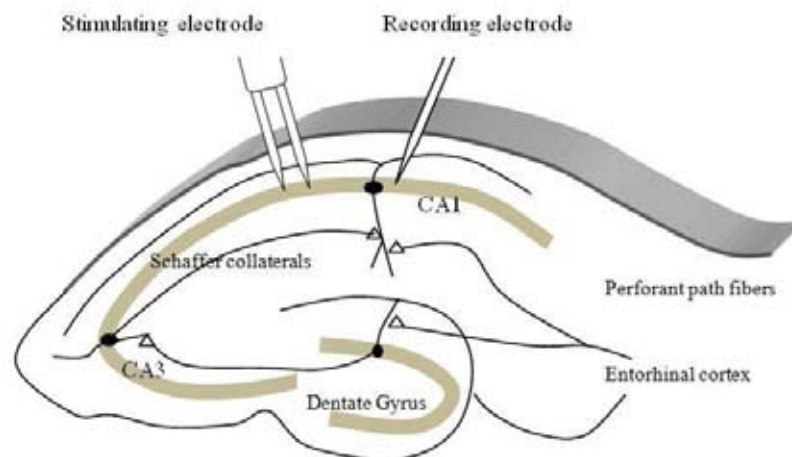


**Figure 3.3** The electrode placement for LTP induction in area CA1 of the hippocampus.

At the start of each experiment, a single square pulse was delivered once every 10 seconds (0.1 Hz) for a test of stimulus. After fEPSPs were acquired and remained stable for at least 30 minutes as the baseline level, the tetanic stimulation or TBS were applied. The tetanic stimulation consisted of 100 pulses in 1 second (100 Hz). TBS is typically consists of three trains of 10 brief 100 Hz bursts, 4 impulses each, 200 msec between burst and is repeated in 10 seconds between train as shown in Figure 3.4. For more detail consult the literature (Albensi *et al.*, 2007; Bongsebandhu-phubhakdi & Manabe, 2007). Finally, I applied a 0.1 Hz test stimulus and continued recording for 60 minutes. LTP was estimated to be the change in slope of the fEPSPs at the final 10 minutes of recording period.



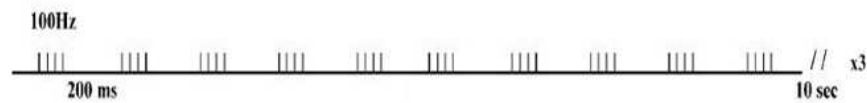


**Figure 3.4** Theta-burst stimulation is typically consisting of three trains of 10 brief 100 Hz burst, 4 impulses each, 200 msec between burst and repeated in 10seconds between train.

### Data Acquisition and Analysis

The recorded signals were amplified, filtered, digitized and transferred to personal computer for online and off-line analysis by Patchmaster multi-channel data acquisition software (HEKA Instruments Inc, Bellmore, New York, USA) as main component show in Figure 3.5.



**Figure 3.5** The main window of HEKA software

The fEPSPs were measured from early time positioned after presynaptic volley and using a time period at about 25 ms. Figure 3.6 is an example of the raw fEPSPs, and the changeability of fEPSPs slope between the arrowheads was used for measuring fEPSP changes from base line as the LTP magnitude.

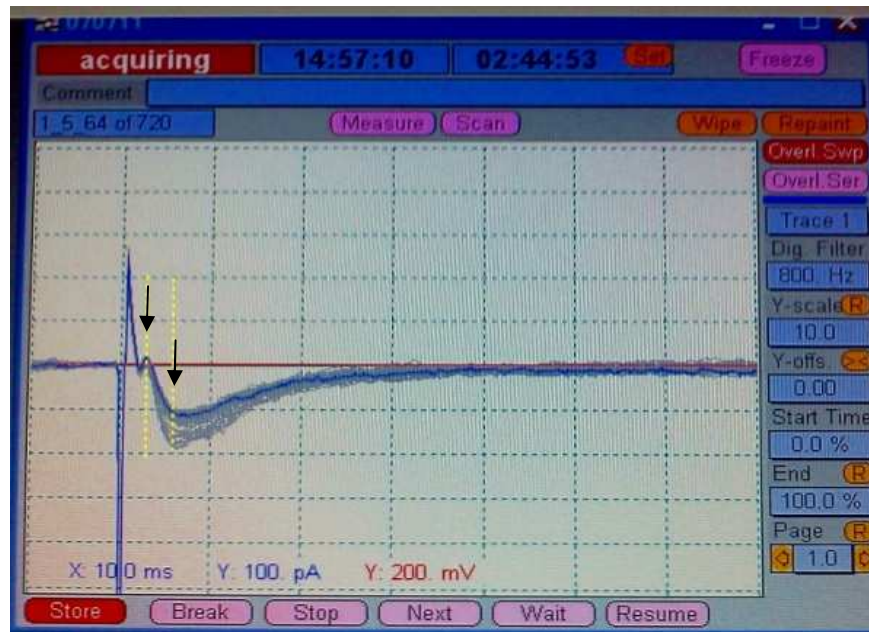


**Figure 3.6** An example of the raw fEPSPs, and the slope between the arrowheads is used for measuring fEPSP changes before and after tetanic stimulation/TBS as the LTP magnitude.

Data obtained in the individual experiments were normalized to their respective baselines that were referenced 100%. The data are expressed as the mean values of the groups and standard errors of the mean values (mean $\pm$ SEM). Statistical comparisons were performed by the analysis of variance test (one-way ANOVA). The  $\alpha$  level for statistical significance was set at  $P < 0.05$ . All computation used Microsoft Excel 2007.

### Least Square Curve Fitting

The purpose of curve fitting is to describe experimental data as mathematical equations. Data are interpreted into a recognized model  $y(t, a_0, a_1, \dots, a_m)$ , where  $y$  is dependent variable which is measurement,  $t$  is independent variable which controlled by the experimenter and  $(m+1)$  variables  $a_0, a_1, \dots, a_m$  are computing parameters from data.

Let  $(t_1, y_1), (t_2, y_2), \dots, (t_n, y_n)$  be given  $n$  data points, least-squares curve fitting problems arise when fitting a parameterized model to real data points by minimizing the sum of squares of error between the data points and this model. Then the objective function for the minimization problem is

$$F(a_0, a_1, \dots, a_m) = \sum_{i=1}^n (y_i - y(t_i, a_0, a_1, \dots, a_m))^2 \quad (3.1)$$

The basic idea for obtaining solution is calculus approach. Technically, the derivative of objective functions with respect to  $a_i, i=0, \dots, m$  equal to zero. Thus parameters  $a_i$  are solved which are substituted in  $y(t, a_0, a_1, \dots, a_m)$  as goodness fitted model. A difference between fitted value provided by model and observed value is residual which considerate to zero as ideally fitting. The computational methods for solving least square problems, we used Levenberg-Marquardt method, see (Leader, 2004: 551-514; Marquard, 1963: 431-441) with Origin-Pro 8.5 software (OriginLab, Northampton, Ma, USA).

The coefficient of determination or  $R^2$  is one measurement effectiveness of an estimated curve fits the data, the formula as

$$R^2 = 1 - \frac{RESS}{Total\ SS} = 1 - \frac{\sum (y - y_{fit})^2}{\sum (y - \bar{y})^2} \quad (3.2)$$

where  $RESS$  is residual sum of squares,  $Total\ SS$  is total sum of squares,  $y$  is values from data,  $y_{fit}$  is fitted values and  $\bar{y}$  is mean of data values.

The  $R^2$  equals the proportion of the total variation in the values of the independent variable, ( $y$ ) that can be explained by the association of  $y$  with  $t$  as measured by the estimated curve (Kohler, 2002: 753-756). If  $R^2$  converge to 1 then modeled with curve fitting more closely corresponded those actually data. In addition the value of  $R^2$  above 0.8 or so are considered good (Dewy, 1994).

For completeness, I assessed the adjusted- $R^2$  or  $R_{adj}^2$  to compensate for practicable bias due to distinct number of parameters (Spiess, 2010: 1-11) as shown in Eq. (3.3)

$$R_{adj}^2 = 1 - (1 - R^2) \left( \frac{q-1}{q-p-1} \right) \quad (3.3)$$

where  $q$  is sample size and  $p$  is the number of parameters.

## CHAPTER IV

### Results

#### Results from the Experiments

##### 1. Experiments for study the electrical stimulate patterns

The Experiments for study patterned stimuli were present in absence of picrotoxin.

The response minimum 30 minutes before tetanic stimulation and theta-burst stimulation (TBS) were normalized and determined as a baseline response. The intensity was  $0.37 \pm 0.0677V$  with tetanic stimulation and  $0.31 \pm 0.0862V$  with TBS. There were no significant differences among groups we examined for stimulation intensity (one-way ANOVA,  $P=0.122$ ). The statistical values and one way-ANOVA analysis are show in Appendix.

The efficacy of tetanic stimulation and TBS were represented as a percent change of baseline fEPSPs slope. The postPTP is record within first 10 minutes and LTP is measured from an average increase of synaptic responses in 50-60 minutes after tetanic stimulation and TBS.

The beginning of tetanic stimulation ( $N=10$ ) resulted in a large, rapidly magnifying post-tetanic potentiation (PTP), with peak approximately 213% of baseline. The potentiating swiftly decayed over the first 5 minutes post tetanic stimulation and then continued to be stable until the end of recording period (60 minutes after tetanic stimulation, Figure 4.1a and Figure 4.2). The LTP was  $134.88 \pm 6.92\%$  of baseline.

To determine the efficacy of LTP from pattern of stimulation, a TBS was applied ( $N=10$ ). TBS also resulted in a large, rapidly magnifying PTP, with peak approximately 193% of baseline. The potentiated response stabilized within 3 minutes after stimulating, and remained stable until the end of recording period (Figure 4.1b and Figure 4.2). The LTP was  $144.42 \pm 6.54\%$  of baseline. There was a significant difference in the magnitude of LTP induced by tetanic stimulation and TBS ( $p < 0.0001$ ). The results shown that TBS effectively induce LTP more than tetanic stimulation; this finding is illustrated in Figure 4.4 and Figure 4.5.

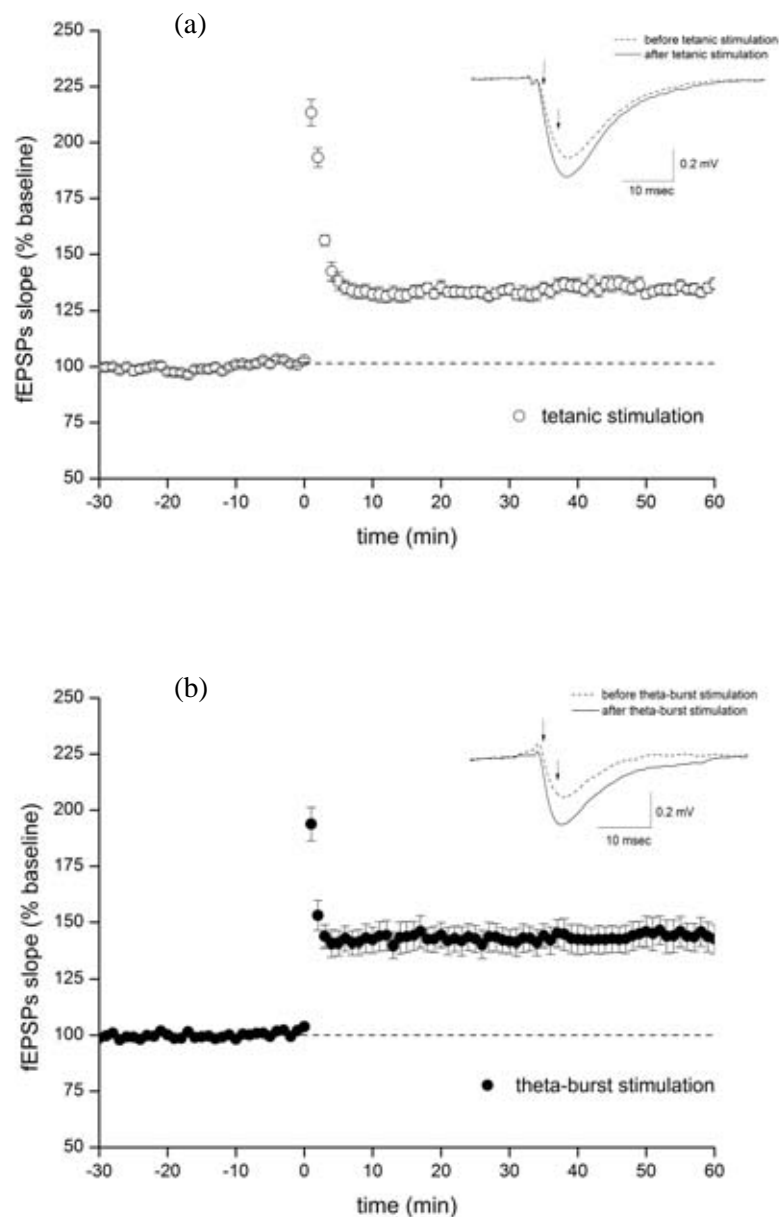


**Figure 4.1** The fEPSPs slope results from tetanic stimulation and theta-burst stimulation. Single-pulse stimuli were delivered every 10 seconds. After a 30 minutes with a stable baseline period (time -30 to 0), either tetanic stimulation or theta-burst stimulation were applied to induce LTP at the 0 time point, and the post tetanic stimulation and theta-burst stimulation responses were continuously recorded for 60 minutes. The measurements of the fEPSP slopes were plotted, for which each point was an average over 6 values of 0.1 Hz (6 points in 1 minute). The inset is an example of the raw fEPSPs, and the slope between the arrowhead is used for measuring fEPSP changes before and after tetanic stimulation and theta-burst stimulation. (a) Tetanic stimulation resulted in rapidly developing LTP that decayed and then stabilized over recording period (LTP was  $134.88 \pm 6.92\%$  of baseline). (b) The theta burst stimulation effectively induce LTP more than tetanic stimulation with  $144.42 \pm 6.54\%$  of baseline.

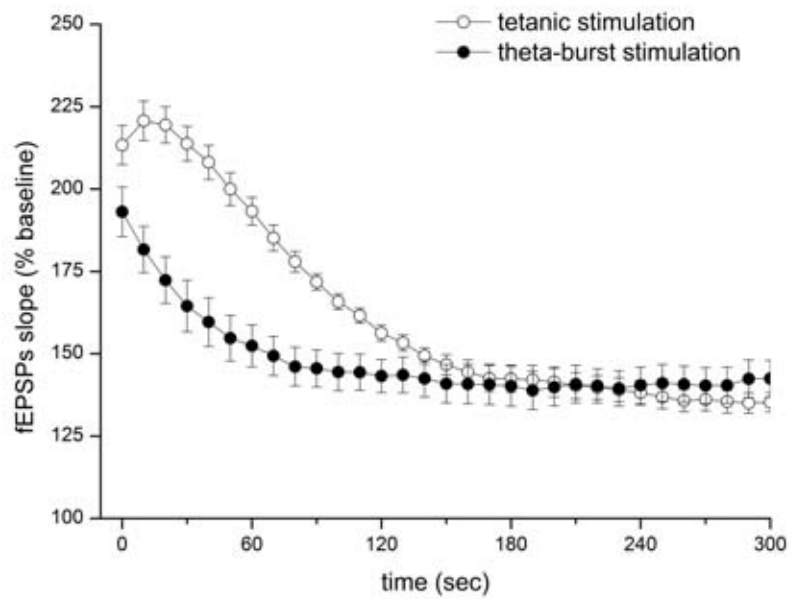


**Figure 4.2** PTP in first 5 minutes after tetanic stimulation and theta-burst stimulation, each point plots 10 seconds time interval.

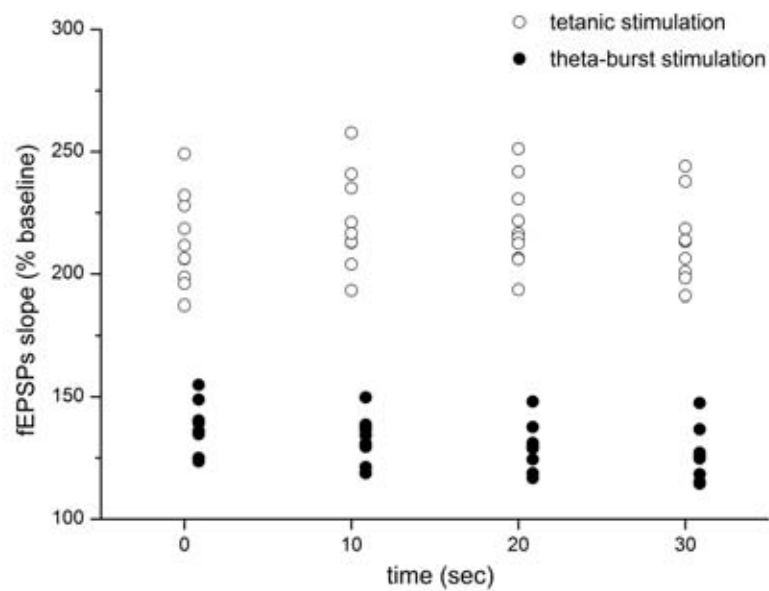


**Figure 4.3** A raw data of fEPSPs slope with N=10 which measured across the first 30 seconds after tetanic stimulation and theta-burst stimulation.

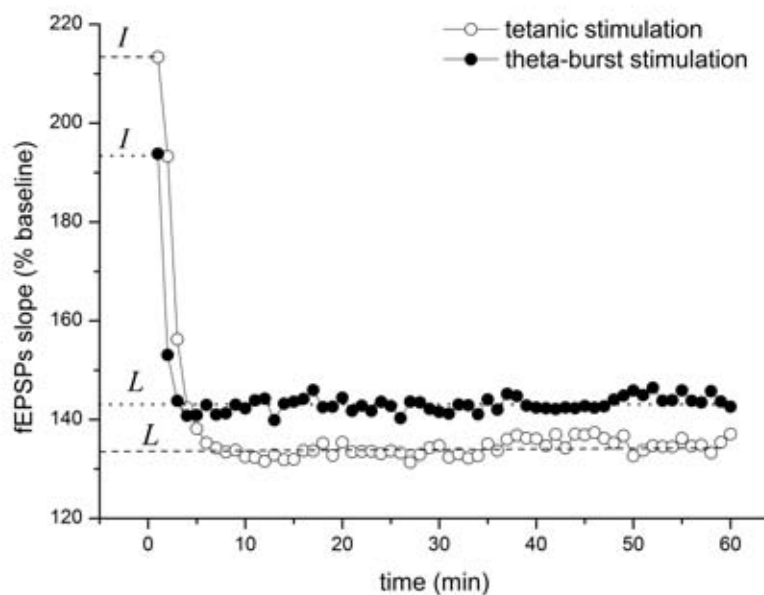


**Figure 4.4** Summary of fEPSPs slope of tetanic stimulation and theta-burst stimulation. The fEPSPs slope in recording period (60 min), *I* and *L* are represented initial and long term response respectively.

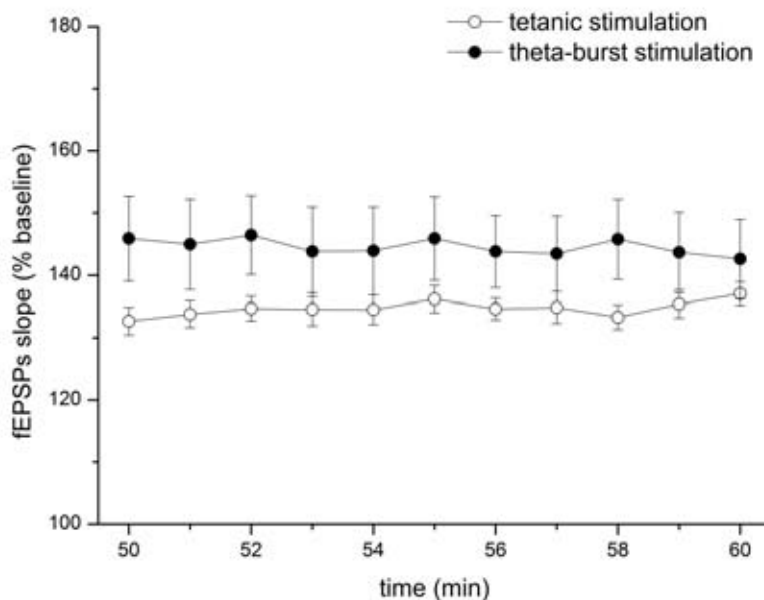


**Figure 4.5** Results of long term potentiations at the final 10 minutes of recording (50-60 min), each point plots the average of fEPSPs slope at interval 1 minute.

## 2. Experiment for study the effect of CSD and Picrotoxin

LTP is also considered to be an average increase in synaptic responses at 50-60 minutes after tetanic stimulation. The largest magnification of PTP was observed in the picrotoxin group (N=8), followed by the picrotoxin+CSD group (N=8) and the control group (N=10, data are same conditions with tetanic stimulation of section1). Then, potentiation swiftly decayed over the first 10 minutes of post-tetanus stimulation and continued stably for the duration of the 60-minute recording period (Figure 4.6, Figure 4.7 and Figure 4.8). The LTP was  $134.88 \pm 6.92\%$  of the baseline in the control group,  $142.25 \pm 4.18\%$  of the baseline in the picrotoxin group and  $120.15 \pm 3.73\%$  of the baseline in the picrotoxin+CSD group (Figure 4.6, Figure 4.7 and Figure 4.9). In all of the groups, there was a significant difference in the amount of LTP,  $p < 0.00001$ .

From all of experiments, the results shown that TBS effectively induces LTP, there are the highest magnitude of LTP as show in Figure 4.10

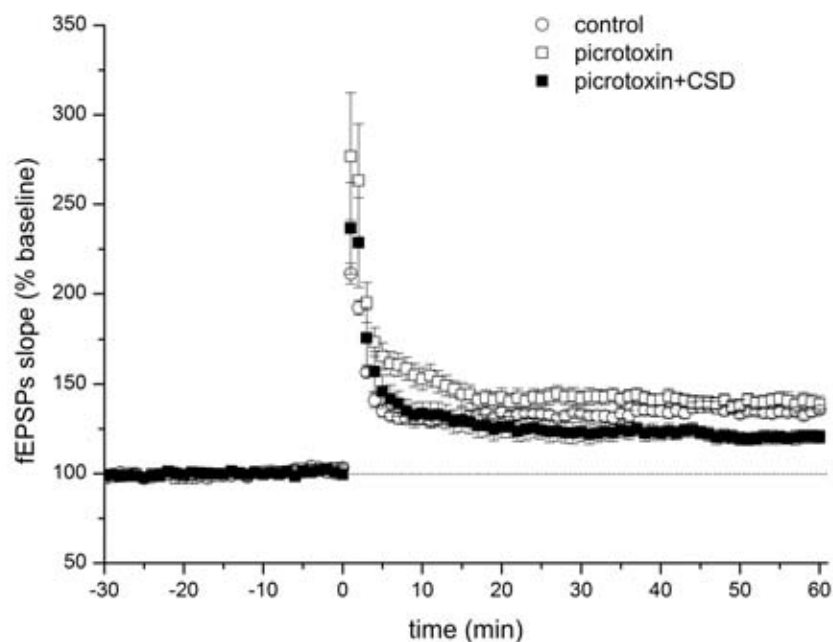


**Figure 4.6** The LTPs were induced under three different conditions. After 30 minutes with a stable baseline period (time -30 to 0), tetanic stimulation was applied at the 0 time point, and the post tetanic responses were continuously recorded for 60 min.



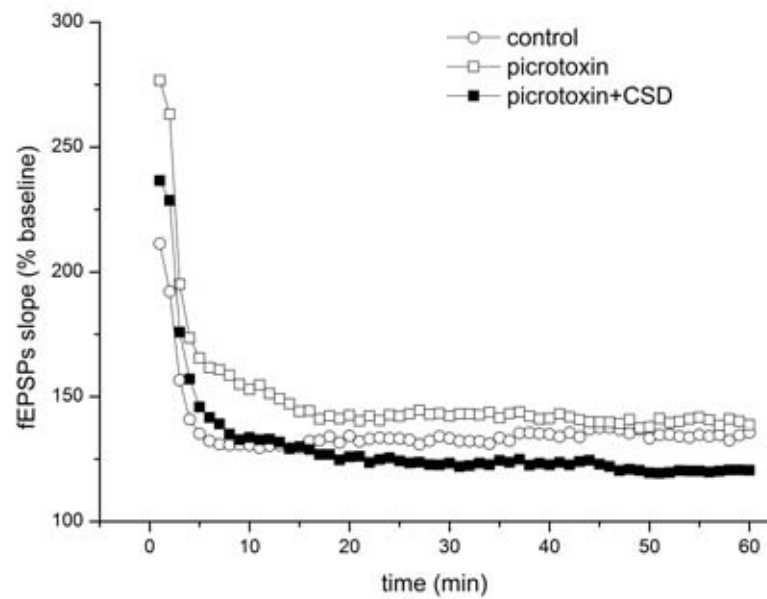


**Figure 4.7** The LTPs were induced under three different conditions. The measurements of the fEPSP slopes were plotted, for which each point was an average over every 6 values of 0.1 Hz (6 points in 1 minute). For the analysis, the error bar were removed and displayed the line for the data relationship.

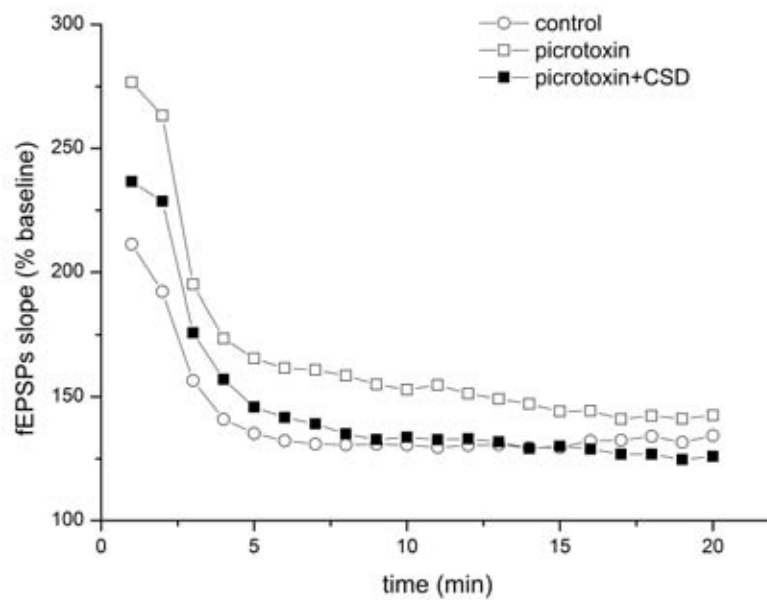


**Figure 4.8** fEPSPs slope in the first 20 minutes after the tetanic stimulation. For the analysis, the error bar were removed and displayed the line for the data relationship.

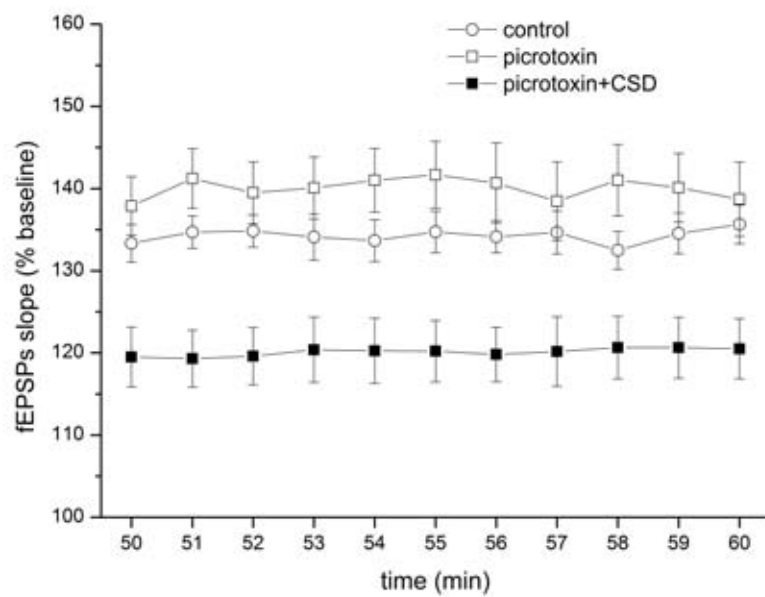


**Figure 4.9** Results of LTPs at the final 10 minutes of recording (50-60 min).

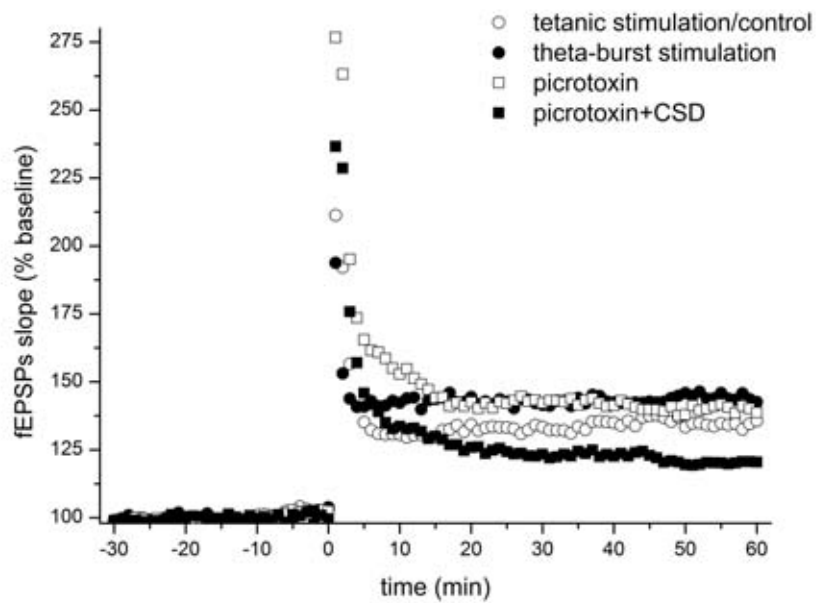


**Figure 4.10** The experimental data of four different conditions. For the analysis, the error bar were removed.

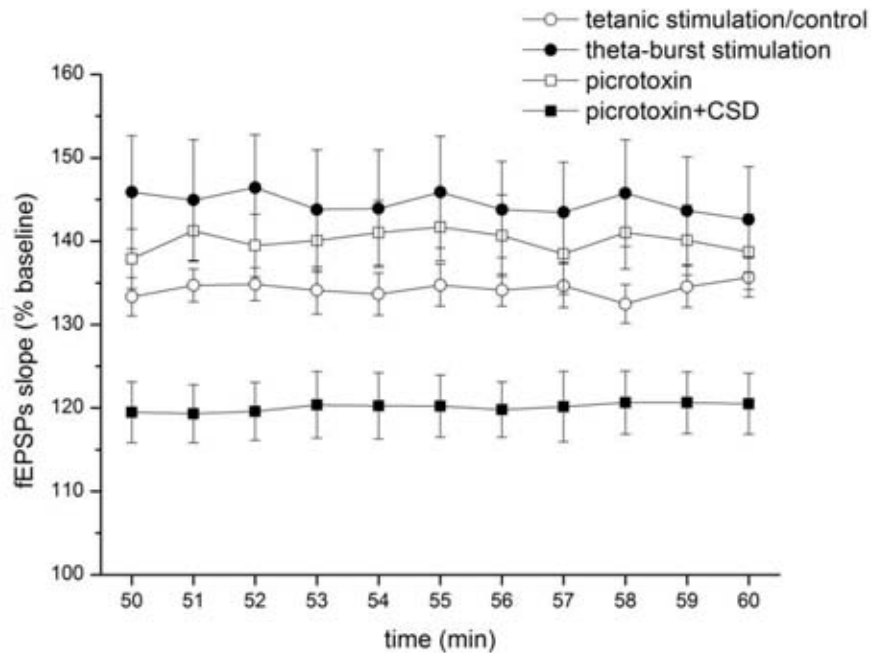


**Figure 4.11** The LTPs were induced under four different conditions.

### Results From Least Squares Curve Fitting

As experimental results above, I considered three models for curve fitting. Since polynomial function is general manipulate for curve fitting because its simplicity of computing, save running time and produced moderately results. We chose polynomial 4<sup>th</sup> order equation for fitted data as

$$y(t) = P_0 + P_1t + P_2t^2 + P_3t^3 + P_4t^4 \quad (4.1)$$

where  $P_0, P_1, \dots, P_4$  are fitting parameters,  $y$  represented % change in the slope of fEPSPs and  $t$  represented times. The least squares curve fitting that was accomplished with a polynomial equation is a linear function which is used to describe the goodness of fit and to make a comparison of the efficacy of each computation.

However the best model could be good explanation of experiments. For the accurate interpretation of experimental results, we concentrated on the percents changes in the fEPSPs after each patterns of stimulation for the magnitude of LTP that was found. This approach resulted in a large PTP that majority of which swiftly decayed over the first 5 minutes and continued to decay over the next 20 minutes. The potentiation then remained stable for the duration of the 60 minute recording period (Figure 4.2, Figure 4.4). Thus these situations produced a second model in exponential equation

$$y(t) = A + Be^{-Ct}, \quad (4.2)$$

where  $y$  is the % change in the slope of fEPSPs and  $t$  is times. All parameter in Eq. (4.2) is reasonable term for data because parameter  $A$  represented stable line and  $Be^{-Ct}$  represented exponential decay curve.

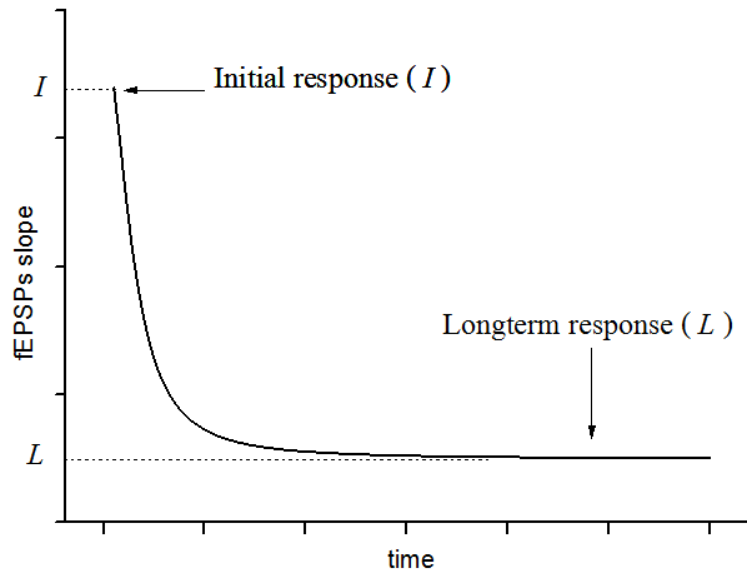


**Figure 4.12** General plot of the data set in arbitrary units.

As displayed in Figure 4.4 and the general plot of data set in Figure 4.12, I determined two relevant time scales of slope of fEPSPs. The initial of PTP, represented by  $I$  and LTP at time 50-60 minutes, represented by  $L$ . We constructed third model with form of power function as follows:

$$y(t) = I \left( \frac{k^n}{k^n + t^n} \right) + L \left( \frac{t^n}{k^n + t^n} \right), \quad (4.3)$$

where  $y$  is the percent change in the slope of fEPSPs,  $t$  is times and  $k, n$  are positive parameters. The power equation in Eq. (4.3) indicates dominant feature of curve in Figure 4.4. This model explained by taking limit of  $t$ , approaching  $0^+$  and  $\infty$  for Eq.(4.3), we obtain

$$\lim_{t \rightarrow 0^+} \left( I \left( \frac{k^n}{k^n + t^n} \right) + L \left( \frac{t^n}{k^n + t^n} \right) \right) = I$$

and

$$\lim_{t \rightarrow \infty} \left( I \left( \frac{k^n}{k^n + t^n} \right) + L \left( \frac{t^n}{k^n + t^n} \right) \right) = L .$$

These limit results are reasonable for experimental data interpretation. Eq. (4.3) was simplified to the following

$$\begin{aligned} y(t) &= \frac{Ik^n + Lt^n}{k^n + t^n} \\ &= \frac{I(k^n + t^n) + Lt^n - It^n}{k^n + t^n} \\ &= I + (L - I) \left( \frac{t^n}{k^n + t^n} \right). \end{aligned}$$

Thus the third model with power function for least square curve fitting is

$$y(t) = I + (L - I) \left( \frac{t^n}{k^n + t^n} \right) \quad (4.4)$$

Note that, the model construction in Eq. (4.2) and Eq. (4.4) are model for the nonlinear least square curve fitting.

For the solving of all parameters  $P_0, P_1, P_2, P_3, P_4$  from Eq. (4.1),  $A, B, C$  from Eq. (4.2) and  $I, L, k, n$  from Eq. (4.4) and recalled from Eq. (3.1), we must minimize the function

$$f = \sum_{i=1}^n (y_i - y(t_i))^2 \quad (4.5)$$

where  $(t_i, y_i), i=1, \dots, n$  are the given  $n$  data points. The parameters of Eq. (4.5) were obtained from fitting the experimental data in recording period (1-60 minutes of after tetanic stimulation and TBS) with OriginPro 8.5 software. The summary of fitting results is shown in table 1. In addition, the values for the fit parameters with the control group, picrotoxin group and picrotoxin+CSD group were obtained. These values are shown in table 2. The curve fitting and residuals (difference value between experiment data and fitting) are shown in Figures 4.13- Figure 4.17.

In accordance with Eq. (4.1), Eq. (4.2) and Eq. (4.4) and the parameter values from table 1 table 2, these allow to calculate the function  $y(t_i)$  at arbitrary time constants and determine magnitude of LTP. The initial PTP,  $y(t_1)$  was calculated by substitute  $t_1 = 1$  (as  $y_1$  in table 3 and table 4). In order to compare with real data  $y_i$ , the relative error was used, with the formula  $|(y_i - y(t_i)) / y_i|$ . Consequently, LTP was calculated from the average of  $y(51), y(52), \dots, y(60)$  and typical results of computational model of fitting LTP are summarized in table 3 and table 4.

**Table 1** The parameters values of least square fitting, with data of stimulated patterns

Models	Parameters	Tetanic stimulation	Theta-burst stimulation
Polynomial equation, $y(t) = P_0 + P_1t + P_2t^2 + P_3t^3 + P_4t^4$	$P_0$	195.52647	165.99986
	$P_1$	-10.88533	-4.19639
	$P_2$	0.58624	0.22911
	$P_3$	-0.01227	-0.00485
	$P_4$	8.79114E-5	3.52476E-5
Exponential equation, $y(t) = A + Be^{-Ct}$	$A$	134.05117	143.06938
	$B$	153.85253	277.08508
	$C$	0.60322	1.69598
Power equation, $y(t) = I + (L - I) \left( \frac{t^n}{k^n + t^n} \right)$	$I$	214.52135	194.24051
	$L$	134.26524	143.08861
	$k$	2.46777	1.70749
	$n$	4.77765	8.94841

**Table 2** The parameters values of least square fitting, with control, Picrotoxin and Picrotoxin+CSD data.

Model	Parameters	Control	Picrotoxin	Picrotoxin+CSD
Polynomial equation	$P_0$	195.52647	262.12361	227.33046
	$P_1$	-10.88533	-18.59255	-15.68811
	$P_2$	0.58624	0.9514	0.79584
	$P_3$	-0.01227	-0.01954	-0.0163
	$P_4$	8.79114E-5	1.38799E-4	1.1555E-4
Exponential equation	$A$	134.05117	142.16181	123.38844
	$B$	153.85253	207.86261	170.21673
	$C$	0.60322	0.38477	0.34942
Power equation	$I$	214.52135	296.19897	253.6417
	$L$	134.26524	141.68052	122.70538
	$k$	2.46777	2.65676	2.82771
	$n$	4.77765	2.42568	2.28393

**Table3** Representative of first PTP of stimulated pattern experiments, comparison between experimental data and computational value; and  $R_{adj}^2$  values.

Models		$R_{adj}^2$	$y_1$	$y(t_1) = y(1)$	Relative errors
Tetanic stimulation	Polynomial	0.69836	213.36324	185.21520	0.131925
	Exponential	0.95751	213.36324	218.21578	0.022743
	Power	0.98484	213.36324	213.46351	0.000470
Theta-burst stimulation	Polynomial	0.32125	193.81808	162.02777	0.164021
	Exponential	0.95216	193.81808	193.89216	0.000382
	Power	0.95247	193.81808	193.81782	0.000001

$y_1$  : experimental data of first PTP,  $y(1)$  : computational value of first PTP

**Table4** Representative LTP of stimulated pattern experiments, comparison between experimental LTP and computational LTP

Model		LTP	Fitting LTP	Relative error
Tetanic stimulation	Polynomial	134.88271	135.04725	0.001220
	Exponential	134.88271	134.05117	0.006165
	Power	134.88271	134.26527	0.004578
Theta-burst stimulation	Polynomial	144.42413	144.72374	0.002074
	Exponential	144.42413	143.06938	0.009380
	Power	144.42413	143.08861	0.009247

LTP: experimental LTP, Fitting LTP: LTP from model fitting

**Table5** Representative of first PTP of control, PicROTOXIN and PicROTOXIN+CSD groups, comparison between experimental data and computational value; and  $R_{adj}^2$  values.

Models		$R_{adj}^2$	$y_1$	$y(t_1) = y(1)$	Relative errors
Control	Polynomial	0.69836	213.36324	185.21520	0.131925
	Exponential	0.95751	213.36324	218.21578	0.022743
	Power	0.98484	213.36324	213.46351	0.000470
PicROTOXIN	Polynomial	0.83387	276.69642	244.46306	0.117363
	Exponential	0.95533	276.69642	283.63459	0.0241066
	Power	0.96867	276.69642	282.99113	0.021743
PicROTOXIN +CSD	Polynomial	0.85031	236.56528	212.42201	0.102056
	Exponential	0.95837	236.56528	243.40773	0.028925
	Power	0.97281	236.56528	242.48966	0.025045

**Table6** Representative LTP of control, PicROTOXIN and PicROTOXIN+CSD groups comparison between experimental LTP and computational LTP

Models		LTP	Fitting LTP	Relative error
Control	Polynomial	134.88271	133.04725	0.001220
	Exponential	134.88271	134.05117	0.006165
	Power	134.88271	134.26527	0.004577
PicROTOXIN	Polynomial	140.24921	139.45302	0.005675
	Exponential	140.24921	142.16181	0.013639
	Power	140.24921	141.77865	0.010907
PicROTOXIN+CSD	Polynomial	120.14960	119.61757	0.004443
	Exponential	120.14960	123.38844	0.026953
	Power	120.14960	122.85266	0.022494



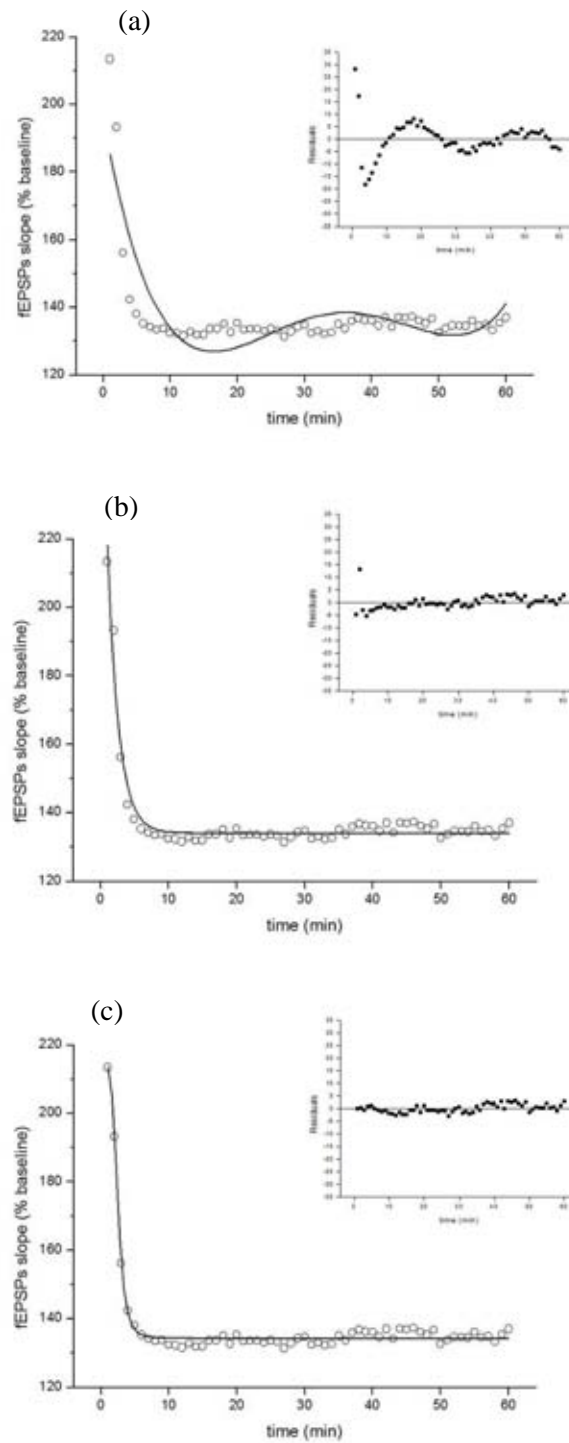


**Figure 4.13** The experimental results of the fEPSPs slope (% baseline) from tetanic stimulation. The lines represent curve fitted with least squares procedure, the insets show residual or error from curve fitting and the exact data. (a) Curve fitting with polynomial model, (b) Curve fitting with exponential model, (c) Curve fitting with power model.

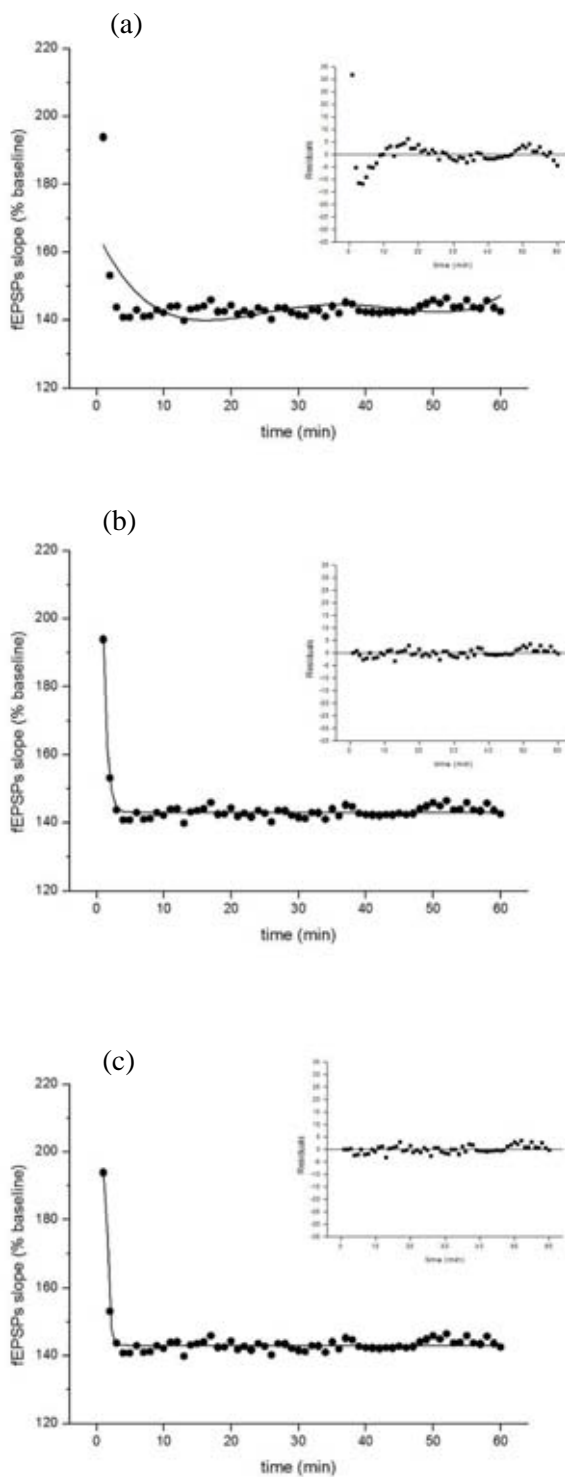


**Figure 4.14** The experimental results of the fEPSPs slope (% baseline) from TBS. The lines represent curve fitted with least squares procedure, the insets show residual or error from curve fitting and the exact data. (a) Curve fitting with polynomial model, (b) Curve fitting with exponential model, (c) Curve fitting with power model.

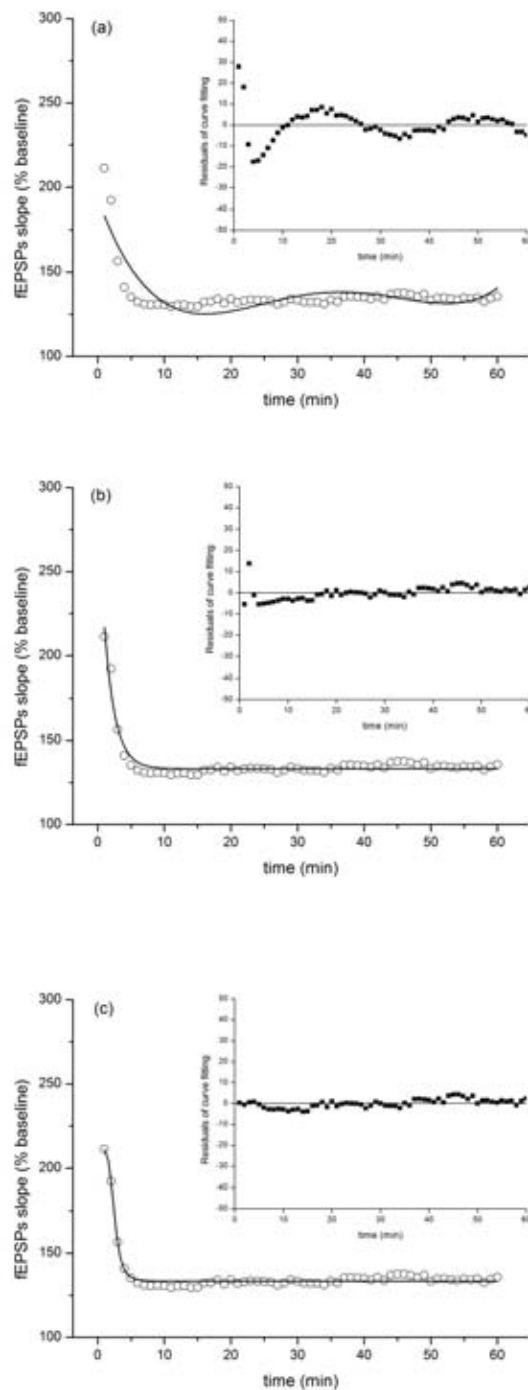


**Figure 4.15** The experimental results of the fEPSP slopes (% baseline) from the control group. The lines represent the results of curve fitting with the nonlinear least squares procedure, the above inset show residuals from fitting. (a) Curve fitting with polynomial model, (b) Curve fitting with exponential model, (c) Curve fitting with power model.

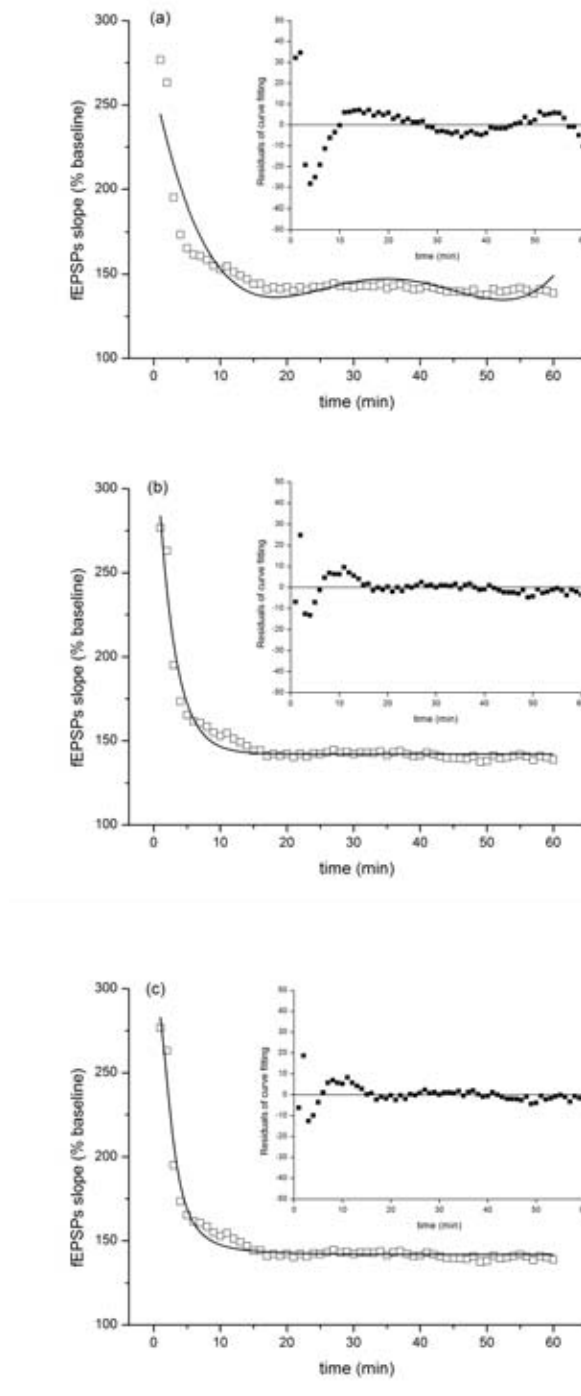


**Figure 4.16** The experimental results of the fEPSP slopes (% baseline) from the picrotoxin group. The lines represent the results of curve fitting with the nonlinear least squares procedure, the above inset show residuals from fitting. (a) Curve fitting with polynomial model, (b) Curve fitting with exponential model, (c) Curve fitting with power model.

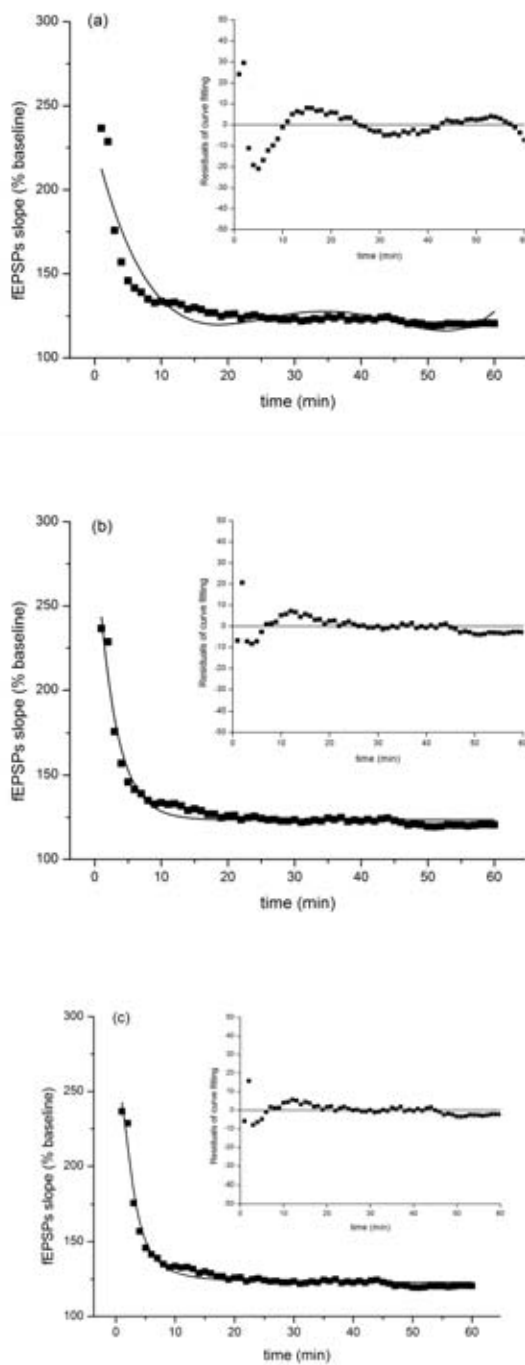


**Figure 4.17** The experimental results of the fEPSP slopes (% baseline) from the picrotoxin+CSD group. The lines represent the results of curve fitting with the nonlinear least squares procedure, the above inset show residuals from fitting. (a) Curve fitting with polynomial model, (b) Curve fitting with exponential model, (c) Curve fitting with power model.

## CHAPTER V

### DISCUSSIONS AND CONCLUSIONS

#### The Efficacy of Nonlinear Least Square Curve Fitting

Curve fitting not only gives a approximation of values that do not appear in the data set but also describes characteristics of the data. For a mathematical description of the model,

the power equation:

$$y(t) = I + (L - I) \left( \frac{t^n}{k^n + t^n} \right),$$

makes it is easy to find the first potentiation and LTP from the values of  $I$  and  $L$ , respectively. In addition, the exponential form  $y(t) = A + Be^{-Ct}$  (Eq. (4.2)) could be an approximation to the fEPSP slopes at a certain time. The LTP approximation was performed by considering a large value for  $t$ . Because  $Be^{-Ct}$  is close to zero when there is a very large value of  $Ct$ , LTP could be estimated by the value of  $A$ .

Moreover, results from the fitting and Eq. (4.2) are intrinsically capable of differential information as a result of the time-dependent changes in the fEPSP slopes. The derivative of

Eq. (4.2) is

$$\frac{dy}{dt} = -CBe^{-Ct} \quad (5.1)$$

Equation (5.1) shows the decay rate of the post tetanus stimulation, whereby there is a decay to a stable value for LTP. This decay might also play a role in short-term plasticity and other time-dependent properties that are involved in changes in synapses. The modifications from Eq. (4.1) and the data in table 2 produce a rate of decay for the post tetanus stimulation shown in Figure 5.1.

Nonlinear systems occur widely in mathematical analysis and often provide a more realistic analysis than can be obtained by using a system of linear equations (Atkinson & Han, 2004; Bielecki & Kalita, 2008; Iannella & Tanaka, 2006; Ude *et al.*, 2009; Ude *et al.*, 2010). This system provided high computational efficacy, which is available to researchers when attempting to make their systems as accurate as possible (Aur *et al.*, 2011; McCullough 2004; Bennani *et al.*, 2009). The potentiation after the tetanic stimulation involves changes in the synaptic efficacy and is present in two states: PTP, which is a short temporal decay in the potential after a stimulation (Zucker, 1989), and LTP, which is the steady state of the potentiation. Our experimental data behaved like the exponential equation in Eq. (4.2). Moreover, Eq. (4.4) is a nonlinear power equation that is produced from an initial ( $I$ ) and

long-term ( $L$ ) potentiation and is modified with a power function. In addition, the polynomial is a basic function for quantifying because it is easy to solve the coefficients with a general computer program. We also quantifies with a polynomial equation for the purpose of comparing the other nonlinear equations. For convenience, the parameters of the least squares quantifying were determined by Origin software.

This research found more accurate fitting results with  $R_{adj}^2$ , which were more than 0.9 with the exponential and power equation, and the run time of the algorithm was approximately 30 seconds. It can be observed that the polynomial equation gave a lower value for  $R_{adj}^2$  compared to the other nonlinear equations.

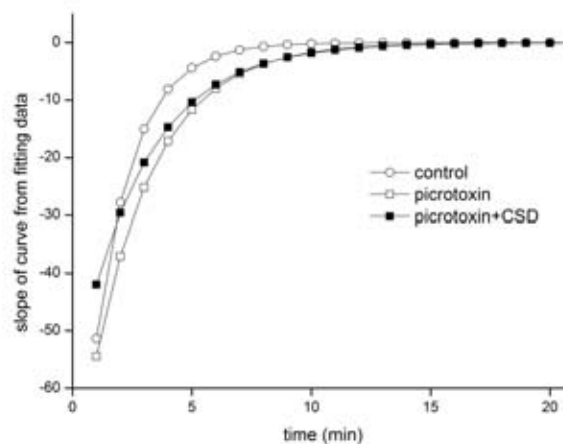


**Figure 5.1** Rate of decay of PTP or the slope from the Eq. (4.2); parameter values in table 2 were used.

### Computational Approach for LTP Describes Their Efficacy of Stimulate Patterns

The present studies reveal that the effects of tetanic stimulation and TBS protocols on synaptic changes and the magnitude of LTP in area CA1 of Hippocampus. The results also show LTP description by least-square curve fitting which enabled us to distinguish between the usefulness of some LTP conditions. While tetanic stimulation have been the favored method for LTP induction, it is not relevant to natural behavior related with learning in the intact animal (Grover et al., 2009: 69; Morgan and Teyley, 2001: 1289; Tsukada, 1994: 495). TBS were created that seem capable of eliciting LTP and naturally closer to what occurs in hippocampus during learning and memory (Abarbanel et al., 2002: 10132; Lynch, 1998: 83).

However, it remains unclear from several studies why LTP magnitude for tetanic stimulation TBS was statistically different (Albensi et al., 2007:1-13).

Hippocampal LTP has been studied as a cellular model of learning and memory (Bliss and Collingridge, 1993; Crozier et al., 2004: 109-122) which is induction by brief high frequency and TBS. Potentiation from induction is divided into three phases; post tetanic potentiation-PTP, an immediately decrease of synaptic efficacy following with a plateau of LTP (Volianskis and Jensen, 2003:459-492). Considerable evidence now connects the increase in postsynaptic  $Ca^{2+}$  to initial steps induction of LTP (Albensi et al., 2007; 1-13; Bear et al., 2007: 776-780). In contrast PTP arising from a presynaptic accumulation of  $Ca^{2+}$  during potential induction and the accelerated decay of PTP reflects a component in removal of residual  $Ca^{2+}$  from the presynaptic terminal (Volianskis and Jensen, 2003; Zucker, 1989).

Because initial PTP from tetanic stimulation is higher than TBS (Figure 4.3), it's suggest that  $Ca^{2+}$  of tetanic stimulation are accumulated in presynaptic terminal more than  $Ca^{2+}$  of TBS. In the same way, a line-scatter plot for individual experiments shown in Figure 4.2, at first 5 minutes provide some interesting observations. It seems that second and third records after tetanic stimulation resulted in slightly larger response compared with first the record. It was remain situate about 30 seconds before rapid decay and it may unseen in recording if stimuli procedure using longer time course, whereas this results not happen in TBS. It also suggests that TBS could be removed presynaptic  $Ca^{2+}$  rapidly than tetanic stimulation. Moreover, our results from the derivative of fitting equation (Eq.(4.1),(4.2),(4.4)), shown a decay rate of PTP that also plays a role in calcium ion, short-term plasticity and other time-dependent properties that are involved in changes in synapses (Langdon et al., 1995: 370-385; Volianskis and Jensen, 2003; Woodson, Schlapfer and Barondes, 1978: 33-46).

From an approximation of initial PTP of tetanic stimulation and TBS as  $y_1$  in table 3, the model of power equation gave the smallest error for  $y_1$ . In contrast the polynomial model produced a relatively high error, and it corresponds to the results, which produced high residuals from the fitting (inset; Figures. 4.13a, 4.14a). These results indicated that the approximation from the polynomial model could be far from the real data. This indication fits our expectation because the exponential and power form model fit from actual PTPs while the polynomial did not.

For LTP description (see the relative error in table 4); although polynomial model gave smallest of relative error but results in higher residuals than the other models (see the last 10 minutes in Figure. 4.13, Figure. 4.14, which show both the positive and negative



residuals in polynomial model). The results suggest that the minimum relative error was calculated from the deletion of positive and negative errors of approximation values. Thus the power equation model could be the best LTP approximation. Moreover, the maximum of the adjusted coefficient of determination was found to be in the power equation model because the main purpose of  $R_{adj}^2$  is the description of future outcomes on the basis of other related data and the model is not specific to certain points. Together, these results, curve fitting with a power equation model are a good choice for overall estimations.

Since different type of stimulation results in different in the magnitude of LTP (Albensi et al., 2007) that our curve fitting technique show TBS produced greater LTP than tetanic stimulation.

What might be the reason why TBS more effective than tetanic stimulation in LTP induction? Research has shown that high frequency stimulation is a conditional requirement for postsynaptic CA1 neuron being strongly depolarized (Albensi et al., 2007; Hernandez et al., 2005; Volianskis and Jensen, 2003). To achieve this depolarization, tetanic stimulation must be stimulated synapse at frequencies high enough to cause temporal summation and spatial summation of EPSP. Moreover, the high frequency activation of synapse is consistent with the mass of synaptic neuropeptide release, whereas LTP induction by TBS is less effective in neuropeptide releasing (Bongsebandhu-phubhakdi and Manabe, 2007).

In addition the optimal theta frequency patterned for the induction of LTP was produced from the burst interval of 200 msec (Larson and Lynch, 1986). The observations from Hernandez et al., conclude that TBS produced greater LTP than 100 Hz with protocols having a pulse number up to 200 or 300, (Hernandez et al., 2005). However I used TBS with total a 120 pulses and curve fitting results show that the TBS protocol is more effective for LTP induction than tetanic stimulation. This explanation suggests specific electrical stimulation patterns give different effect to LTP.

### **Computational Approach of Altered LTP That Used to Investigated the Effects of CSD and Picrotoxin on the Synaptic Plasticity**

The initial response of tetanic potentiation is a very high magnitude from the baseline, and it swiftly decays, which is approximated as  $y(1)$  in table 5. The model of power equation gave the smallest relative error for  $y(1)$  in all of the experimental groups. The polynomial equation produced a relatively high error, and it corresponds to the data in Figures. 4.15-4.17, which produced high residuals from the fitting (Figures. 4.15a, 4.16a, 4.17a). These results

indicated that the approximation from the polynomial equation could be far from the real data. This indication fits our expectation because the exponential and power equation fit from actual PTPs while the polynomial did not. An interesting algorithm from Philipp (Spitzer *et al.*, 2006) fits multiple measured data simultaneously and results in increasing the parameter accuracy.

Next, we focused on LTP computation (see the LTP, Fitting LTP and relative error in table 6). Although the polynomial equation gave the smallest relative errors, the LTP computation of all equations resulted in quite similar values when comparing experimental LTP and quantifying LTP. In contrast, the polynomial equation gave higher residuals than the other equations (see the last 10 minutes in inset of Figures 4.15a, 4.16a, and 4.17a which show both the positive and negative residuals). The results suggest that the minimum relative error was calculated from the deletion of positive and negative approximation values.

In accordance with the computational values and the functions obtained from fitting, it is difficult to determine a mathematical equation of the experimental investigations that could be best described as the potentiation from the tetanic stimulation, especially LTP. With respect to the best equation based on the minimum relative error, each equation can reproduce the experimental data for a different case. However, the maximum of the adjusted coefficient of determination was found to be in the power equation because the main purpose of  $R_{adj}^2$  is the prediction of future outcomes on the basis of other related data; the technique is not specific to certain points. Moreover, quantifying with a power equation is a good choice for overall estimations.

The results of fitting to suitable mathematical expressions could be important factors related to real neuronal plasticity. Little information is available on the mechanisms that underlie the initiation and propagation of CSD. Ionotropic glutamate receptor channels have been proposed to play a role (Gorji, 2001; Mody *et al.*, 1987; Wernsmann *et al.*, 2006). AMPA receptors quickly desensitize and therefore do not contribute substantially. NMDA receptors are regularly blocked by magnesium at resting potential, and CSD depolarization is expected to relieve the block. Traditional studies investigated that glutamate can trigger CSD (Coan & Collingridge, 1985; Edelstein & Mauskop, 2009; Rogawski, 2012; Van & Fifkova, 1973). Moreover, they demonstrated that glutamate-induced CSD was found to be inhibited while occurring in high concentrations of magnesium ions (Rogawski, 2012).

Of course, glutamate is known to be involved in excitatory synapses, while GABA<sub>A</sub> acts at inhibitory synapses in the brain. Therefore, GABA<sub>A</sub> antagonists could increase PTP and LTP (Albeni *et al.*, 2007). Within slice comparisons between potentiation in the

microtoxin group and the control group (Figure 4.8), I showed a greater fEPSP response of the microtoxin group at initial PTP. This observation corresponds to the quantifying application in which the synaptic responses in the microtoxin group were obviously higher than in the control group for the first 5 minutes.

In addition, tetanic stimulation was delivered to area CA1 of hippocampus tissues after induced CSD. Initial PTP in the microtoxin+CSD group resulted in a higher baseline compared with the control group. This augmentation resulted from the effect of microtoxin. In the long run, CSD resulted in decreasing fEPSPs because glutamate receptors were desensitized. This desensitization could be a majority of the attenuated LTP in the microtoxin+CSD group.

It was obvious that microtoxin could increase LTP and excitability. In contrast, LTP was significantly reduced when applied to CSD because glutamate was desensitized, especially in the microtoxin+CSD group, which showed minimal LTP. The experimental data of this study also revealed the important role of glutamate receptors in the induction of LTP and in synaptic plasticity properties, whereas GABA<sub>A</sub> receptors play a role as a supplementary circuit.

I made two interesting observations from PTP and the slope from our equations. First, in the presence of microtoxin, the CSD produced the slope of the quantified data, the first potentiation value and LTP lower than when CSD was not applied (Figure 5.1). These observations suggest that the decay rate of PTP has a direct relationship with LTP and that this rate might correspond to a desensitization of the glutamate receptors. Second, in the presence of microtoxin, effective PTP occurred by the increase in postsynaptic excitability. This scenario was a direct relationship of the decay-rate, rapid potentiation and LTP. However, the time course of exponential decay to a stable period was maximal with the action of microtoxin compared with the action of CSD (Figure 5.1). The mechanisms of glutamate receptor desensitization by CSD were more powerful than the action of the GABA<sub>A</sub> receptors.

## Conclusions

In this study, proposed model of LTP that provides an experimental results for investigating synaptic plasticity under two conditions: with picrotoxin and with applied CSD before hippocampal slice preparation. In addition I also investigated the efficacy of electrical stimulates patterns of LTP induction: tetanic stimulation and TBS. Thus the TBS produced greater LTP than tetanus stimulation. LTP in CSD group induced by tetanic stimulation was significantly reduced, compared to control group. Picrotoxin effected to increased fEPSP and LTP. Initials posttetanic stimulation in CSD and control group resulted in higher baseline when compared against all other protocols cause from picrotoxin. In long time CSD occurrence results in decreasing fEPSP because of glutamate was desensitized.

The nonlinear least square curve fitting accomplished the goal because it gave the increasable accuracy of parameters. The results shown that the curve fitting with the power equation is the most appropriate model for overall estimations when compared with model of polynomial and exponential equation.

In conclusion, this computation procedure can quantify the alteration of LTP under various conditions. With respect to our findings, both change in excitability from a GABA<sub>A</sub> antagonist and the occurrence of CSD have a definitive effect on the magnitude of LTP.

## REFERENCES

- Abarbanel, H.D.I., Huerta, R., Rabinovich, M.I. (2002). Dynamical model of long-term synaptic plasticity. Proc. Natl. Acad Sci. USA. 99: 10132-10137.
- Albensi, B.C., Oliver, D.R., Toupin, J., Odero, G. (2007). Electrical stimulation protocols for hippocampal synaptic plasticity and neuronal hyper excitability, Are they effective or relevant? Exp. Neurol. 204: 1-13.
- Atkinson, K., Han, W. (2004). Numerical linear algebra advanced topics. Elementary numerical analysis, 3<sup>rd</sup> ed., pp 352-362. New York: John Wiley.
- Bear, M.F., Connors, B.W., Paradiso, M.A. (2007). Neuroscience-exploring the brain, 3<sup>rd</sup> ed., pp 776-780. Philadelphia: Lippincott William & Wilkins.
- Berger, T.W., Sheu, B.J., Tsait, R.H. (1994). Analog VLSI implementation of a nonlinear systems model of the hippocampal brain region. Cellular Neural Networks and their Applications, 1994-CNNA94-Proceedings of the Third IEEE International Workshop on, pp 47-51.
- Bielecki, A., Kalita, P. (2008). Model of neurotransmitter fast transport in axon terminal of presynaptic neuron. J. Math. Biol. 56: 559-576.
- Bliss, T.V., Collingridge, G.L. (1993). A synaptic model of memory, Long-term potentiation in the hippocampus. Nature. 361: 31-39.
- Bongsebandhu-phubhakdi, S., Manabe, T. (2007). The neuropeptide nociceptin is a synaptically released endogenous inhibitor of hippocampal long-term potentiation. J. Neurosci. 27: 4850-4858
- Borkum, J.M. (2007). Chronic headaches-biology, psychology and behavioral treatment. New Jersey: Lawrence Erlbaum.
- Brodal, P. (2010). The central nervous system structure and function. 4<sup>th</sup> ed. New York: Oxford university press.
- Coan, E.J., Collingridge, G.L. (1985). Magnesium ions block an N-methyl-D-aspartate receptor-mediated component of synaptic transmission in rat hippocampus. Neurosci. Lett. 53:21-26.
- Connor, B.W. (2009). Synaptic transmission in the nervous system: Medical physiology. 2<sup>nd</sup> ed. Philadelphia: Saunders Elsevier.
- Crozier, R.A., Philpot, B.D., Sawtell, N.B., Bear, M.F. (2004). Long-term plasticity of glutamatergic synaptic transmission in the cerebral cortex: The Connective Neuroscience. Cambridge MA: MIT press.

- Dehbandi, S., Speckmann, E.J., Pape, H.C., Gorji, A. (2008). Cortical spreading depression modulates synaptic transmission of the rat lateral amygdale. Eur. J. Neurosci. 27: 2057-2065.
- Dewy B.R. (1994). Introduction to Engineering Computing. Columbus OH: McGraw-Hill Primus. XL1-XL20.
- Edelstein, C.S., Mauskop, A. (2009). Role of magnesium in the pathogenesis and treatment of migraine. Expert. Rev. Neurother. 9: 369-379.
- Feder, R., Ranck, Jr. (1973). Studies on single neurons in dorsal hippocampal formation and septum in unrestrained rats II: Hippocampal slow waves and theta cell firing during bar pressing and other behaviors. Exp. Neurol. 41: 532–555.
- Furukawa, K., Sopher, B.L., Rydel, R.E., Begley, J.G., Pham, D.G., Martin, G.M., Fox, M., Mattson, M.P., (1996). Increased activity-regulating and neuroprotective efficacy of alpha-secretase-derived secreted amyloid precursor protein conferred by a C-terminal heparin-binding domain. J. Neurochem. 67: 1882–1896.
- Gorji, A. (2001). Spreading depression-a review of the clinical relevance. Brain Res. Rev. 38: 33-60.
- Grastyan, E., Lissak, K., Madarasz, I., Donhoffer, H., (1959). Hippocampal electrical activity during the development of conditioned reflexes. Electroencephalogr. Clin. Neurophysiol. Suppl. 11: 409–430.
- Graves, A.B., White, E., Koepsell, T.D., Reifler, B.V., vanBelle, G., Larson, E.B., Raskind, M., (1990). The association between head trauma and Alzheimer's disease. Am. J. Epidemiol. 131: 491–501.
- Grover, L.M., Kim, E., Cooke, J.D., Holmes, W.R. (2009). LTP in hippocampal 1 area CA is induced by burst stimulation over broad frequency range centered around delta. Learn. Mem. 16: 69-81.
- Guyton, A.C., Hall, J.E. (2006). Textbook of medical physiology, 11<sup>st</sup> ed. Philadelphia: Elsevier Saunder.
- Hernandez, R.V., Navarro, M.M., Rodriguez, W.A., Martinez, Jr. J.L., LeBaron, R.G. (2005). Differences in the magnitude of long-term potentiation produced by theta burst and high frequency stimulation protocols matched in stimulus number (Protocol). Brain Res. Brain. Res. Protoc. 15: 6-13.
- Holmes, W.R., Ambros, J.I., Grover, L.M. (2006). Fitting experimental data to models that use morphological data from public database. J. comput. Neurosci. 20: 349-365.
- Holmes, W.R., Grover, L.M. (2006). Quantifying the magnitude of changes in synaptic level parameters with long-term potentiation. J. Neurophysiol. 96: 1478-1491.

- Huang, F.S., (2010). Short-and long-term neuronal plasticity in hippocampal CA1 region of rat. Doctoral dissertation, Department of Medical Biophysics, Institute of Neuroscience and Physiology at Sahlgrenska Academy, University of Gothenburg.
- Jedlicka, P. (2002). Review synaptic plasticity, metaplasticity and bcm theory. Bratisl Lek Listy. 4:137-143.
- Kandel, E.R., Schwartz, J.H., Jessell, T.M. (2000). Principles of neural science. 4<sup>th</sup> ed. New York: McGraw-Hill.
- Kandel, E.R., Spencer, W.A. (1961). Electrophysiology of hippocampal neurons II: Afterpotentials and repetitive firing. J. Neurophysiol. 24: 243–259.
- Kandel, E.R., Spencer, W.A., Brinley, Jr. F.J., (1961). Electrophysiology of hippocampal neurons I: Sequential invasion and synaptic organization. J. Neurophysiol. 24: 225–242.
- Kohler, H. (2002). Statistics for business and economics. London: Thomson Learning.
- Langdon, R.B., Johnson, J.W., Barrionuevo, G. (1995). Posttetanic potentiation and presynaptically induced long-term potentiation at the mossy fiber synapse in rat hippocampus. J. neurobiol. 26: 370-385.
- Larkman, A.U., Jack, J.J.B. (1995). Synaptic plasticity hippocampal LTP, Curr. Opin. Neurobiol. 5: 324-334.
- Larson, J., Lynch, G. (1986). Induction of synaptic potentiation in hippocampus by patterned stimulation involves two events. Science. 232: 985-988.
- Lauritzen, M. (1994). Pathophysiology of the migraine aura :the spreading depression theory. Brain. 117: 199-210.
- Leader, J.J. (2004). Numerical analysis and scientific computation. New Jersey: Peason Education.
- Lee, J.S., Ho, W.K., Lee, S.H. (2010). Post-tetanic increase in the fast-releasing synaptic vesicle pool at the expense of the slowly releasing pool. J. Gen. Physiol. 136: 259–272.
- Leao, A.A.P. (1944). Spreading depression of activity in the cerebral cortex. J. Neurophysiol. 7: 359–390.
- Leao, A.P., Morrison, R.S. (1945). Propagation of spreading cortical depression. J. Neurophysio. 8: 33–45.
- Lynch, G. (1998). Memory and the brain: unexpected chemistries and a new pharmacology. Neurobiol. Learn. Mem. 70:82-100.
- Malenka, R.C. (2002). Neuropsychopharmacology 5<sup>th</sup> generation of progress: Synaptic plasticity. New York: Lippincott Williams and Wilkins.

- Manninen, T., Hituri, K., Kotaleski, J.H., Blackwell, K.T., Linne, M.L. (2010). Postsynaptic signal transduction models for long-term potentiation and depression. Front. Comput. Neurosci. 4: 1-29.
- Marquard, D.W. (1963). An algorithm for least-squares estimation of nonlinear parameters. J. Soc. Ind. Appl. Math. 2: 431-441.
- McCullough, B.D. (2004). Some details of nonlinear estimation: Numerical issues in statistical computing for the social scientist. New Jersey: John Wiley.
- Miglior, M., Alicata, F., Ayala, G.F. (1995). A model for long-term potentiation and depression. J. comput. Neurosci. 2: 335-343.
- Migliore, M., Lansky, P. (1999). Long-term potentiation and depression induced by a stochastic conditioning of a model synapse. Biophys. J. 77:1234-1243.
- Mody, I., Lambert, J.D., Heinemann, U. (1987). Low extracellular magnesium induces epileptiform activity and spreading depression in rat hippocampal slices. J. Neurophysiol. 57: 869-888.
- Morgan, S.L., Teyley, T.J. (2001). Electrical stimuli patterned after the theta-rhythm induce multiple forms of LTP. J. Neurophysiol. 86: 1289-1296.
- Nieus, T., Sola, E., Mapelli, J., Saftenku, E., Rossi, P., D'Angelo, E. (2006). LTP regulates burst initiation and frequency at Mossy fiber-granule cell synapses of rat cerebellum: Experimental observations and theoretical predictions. J. Neurophysiol. 95:686-699.
- Olsen, R.W. (2006). Picrotoxin-like channel blockers of GABA<sub>A</sub> receptors. PNAS. 103: 6081-6082.
- Pavlidis, C., Greenstein, Y.J., Grudman, M., Winson, J. (1988). Long-term potentiation in the dentate gyrus is induced preferentially on the positive phase of theta-rhythm. Brain. Res. 439: 383-387.
- Ranck, Jr. J.B. (1973). Studies on single neurons in dorsal hippocampal formation and septum in unrestrained rats I: Behavioral correlates and firing repertoires. Exp. Neurol. 41: 461-531.
- Rogawski, M.A. (2012). Migraine and epilepsy-shared mechanisms within the family of episodic disorders. Jasper's Basic Mechanisms of the Epilepsies. 4<sup>th</sup> ed. New York: Oxford university press.
- Sargsyan, A.R., Papatheodoropoulos, C., Kostopoulos, G.K. (2001). Modeling of evoked field potentials in hippocampal CA1 area describes their dependence on NMDA and GABA receptors. J. Neurosci. Methods. 104: 143-153.
- Somjen, G.G. (2005). Aristides Leao's discovery of cortical spreading depression. J. Neurophysiol. 94: 2-4.



- Song, D., Wang, Z., Marmarelis, V.Z., Berger, T.W. (2009). Parametric and non-parametric modeling of short-term synaptic plasticity: Part II experimental study. J. Comput. Neurosci. 26: 21–37.
- Spiess, A.N., Neumeyer, N. (2010). An evaluation of R2 as an inadequate measure for nonlinear models in pharmacological and biochemical research—a Monte Carlo approach. BMC Pharmacol. 10: 1-11.
- Spitzer, P., Zierhofer, C., Hochmair, E. (2006). Algorithm for multi-curve-fitting with shared parameters and a possible application in evoked compound action potential. Biomed. Eng. Online. 5:13.
- Squire, L. R. (1992). Memory and the hippocampus: A synthesis from findings with rats, monkeys and humans. Psychol. Rev. 99:195-231.
- Tang, Y., Zucker, R.S. (1997). Mitochondrial involvement in post-tetanic potentiation of synaptic transmission. Neuron. 18: 483–491.
- Thomas, P.J., Cowan, J.D. (2011). Generalized spin model for coupled cortical feature maps obtained by coarse graining correlation based synaptic learning rules. J. Math. Biol. DOI 10.1007/s00285-011-0484-7.
- Tsukada, M., Aihara, T., Mizuno, M., Kato, H., Ito, K. (1994). Temporal pattern sensitivity of long-term potentiation in hippocampal CA1 neurons. Biol. Cybern. 70:495-503.
- Ude, L., Dong, S., Theodore, B.W. (2009). Nonlinear model of single hippocampal neuron with dynamical thresholds. Conf. Proc. IEEE. Eng. Med. Biol. Soc. 2009, pp 3330-3334, Minnesota, USA, 2009.
- Ude L, Dong S, Theodore BW (2010) Nonlinear dynamic analyses of single hippocampal neurons before and after long-term potentiation. Conf. Proc. IEEE. Eng. Med. Biol. Soc. 2010, pp 2762-2765, Buenos Aires, Argentina, 2010.
- Van, H.A., Fifkova, E. (1973) Mechanisms involved in spreading depression. J. Neurobiol. 4: 375–387.
- Volianskis, A., Jensen, M.S. (2003). Transient and sustained types of long-term potentiation in the CA1 area of the rat hippocampus. J. Physiol. 550: 459-492.
- Wernsmann, B., Pape, H.C., Speckmann, E.J., Gorji, A. (2006). Effect of cortical spreading depression on synaptic transmission of rat hippocampal tissues. Eur. J. Neurosci. 23:1103–1110.
- Winson, J. (1972). Interspecies differences in the occurrence of theta. Behav. Biol. 7:479–487.

- Woodson, P.B.J., Schlapfer, W.T., Barondes, S.H. (1978). Amplitude and rate of decay of post-tetanic potentiation are controlled by different mechanisms. Brain Res. 157: 33-46.
- Zucker, R.S. (1989). Short-term synaptic plasticity. Ann. Rev. Neurosci. 12: 13-31.

## **APPENDICES**

**APPENDIX A**

## Descriptions of the Results

In this thesis, data of LTP magnitude was estimated to be the change in slope of the fEPSPs. Figure A1 is example of raw data. When a test stimulus was delivered with a single square pulse once every 10 seconds (0.1 Hz), the baseline period of fEPSPs slope was plotted at time -30 to 0. The tetanus stimulation or theta-burst stimulation was applied at time 0 and then applied immediately with a 0.1 Hz test stimulus again. These results were plotted at time 0 to 60 and each points were also 10 seconds interval.

However there are distinct values of the raw fEPSPs slope. For data synchronized, the fEPSPs slope values were averaged and plotted as the percent change from baseline and were referenced 100% as shown in Figure A2. Each points were 1 minute interval.

When data were collected completely in once experimental group, there were averaged as mean value from all experimental data within groups. The mean of the fEPSPs slope (% from baseline) are summarized in table A1.

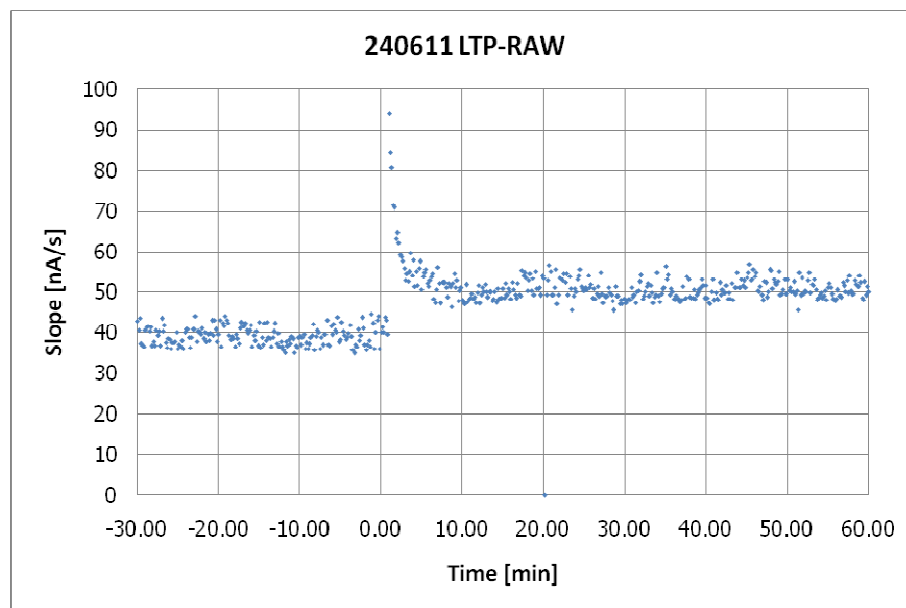


**Figure A1** The example of raw data of the fEPSPs slope

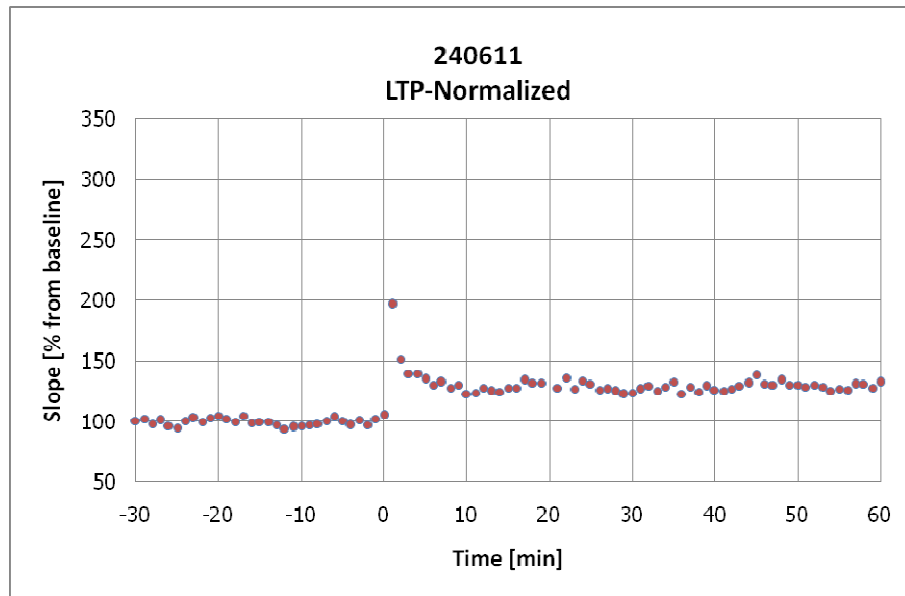


**Figure A2** The example of normalized data of the fEPSPs slope

**Table A1** The mean of the fEPSPs slope (% from baseline)

Time (min)	fEPSPs slope (% from baseline)			
	Theta-burst stimulation	Tetanic stimulation/control	Picrotoxin	Picrotoxin+CSD
-30	98.700	99.669	97.562	99.005
-29	99.745	99.823	98.106	99.333
-28	100.950	99.986	98.392	98.587
-27	97.943	98.562	100.156	99.103
-26	99.336	99.900	99.612	98.617
-25	99.207	98.252	97.652	97.801
-24	98.181	99.006	99.749	98.897
-23	99.897	99.627	98.575	99.192
-22	99.579	100.494	100.901	101.210
-21	101.869	100.348	97.339	99.990
-20	100.196	97.805	97.387	99.512

**Table A1 (Continued)**

Time (min)	fEPSPs slope (% from baseline)			
	Theta-burst stimulation	Tetanic stimulation/control	Picrotoxin	Picrotoxin+CSD
-19	98.608	97.531	97.214	100.652
-18	98.701	97.332	99.762	100.451
-17	101.561	96.405	99.915	100.182
-16	99.040	98.729	98.659	99.937
-15	99.306	99.043	99.759	99.869
-14	99.636	98.956	101.351	101.115
-13	98.406	99.805	100.263	99.907
-12	99.127	98.154	98.700	99.608
-11	100.167	99.782	100.777	100.830
-10	98.279	101.001	99.599	99.870
-9	100.496	101.390	101.256	100.333
-8	100.143	100.787	100.369	99.548
-7	100.857	101.538	101.102	101.147
-6	100.941	102.890	101.652	98.475
-5	99.475	101.350	102.821	101.193
-4	101.863	103.511	102.025	100.794
-3	102.326	103.104	101.427	102.038
-2	99.499	101.303	102.400	102.680
-1	102.098	100.970	103.048	100.955
0	103.868	102.945	102.470	99.579
1	193.818	213.363	276.696	236.565
2	153.080	193.273	263.206	228.617
3	143.781	156.218	195.075	175.806
4	140.772	142.384	173.534	157.029
5	140.882	138.137	165.473	145.853
6	142.937	135.256	161.565	141.615
7	141.002	134.214	160.825	139.033
8	141.274	133.423	158.572	134.994
9	143.017	133.810	154.981	132.736
10	142.268	132.480	152.877	133.657
11	143.893	132.319	154.719	132.687
12	144.231	131.572	151.262	133.004
13	139.874	132.851	149.113	131.772
14	143.205	131.893	147.117	129.082
15	143.620	131.947	144.064	130.007

**Table A1 (Continued)**

Time (min)	fEPSPs slope (% from baseline)			
	Theta-burst stimulation	Tetanic stimulation/control	Picrotoxin	Picrotoxin+CSD
16	144.161	133.714	144.350	128.845
17	145.953	133.681	141.010	126.820
18	142.496	135.232	142.307	126.818
19	142.582	132.742	141.116	124.676
20	144.403	135.388	142.517	125.932
21	141.772	133.469	140.221	126.082
22	142.803	133.559	142.260	123.597
23	141.742	133.566	140.454	124.865
24	143.580	133.084	142.637	125.526
25	142.741	133.678	142.111	124.288
26	140.293	133.255	143.103	123.453
27	143.617	131.345	144.581	123.701
28	143.471	132.923	142.856	122.765
29	142.140	134.287	143.279	122.672
30	141.537	134.749	142.182	123.375
31	141.191	132.365	143.099	121.952
32	143.043	133.030	143.072	122.389
33	142.882	132.191	142.711	123.353
34	141.084	132.686	143.768	122.728
35	144.068	135.081	141.499	124.464
36	142.019	133.687	143.212	123.637
37	145.198	135.987	143.866	124.882
38	144.757	136.825	142.139	122.506
39	142.814	136.241	141.004	123.304
40	142.432	136.090	141.257	122.625
41	142.287	134.696	143.084	123.668
42	142.111	137.009	141.843	122.658
43	142.441	134.256	140.760	123.999
44	142.299	137.074	139.829	124.492
45	142.738	136.876	139.788	122.923
46	142.401	137.353	139.741	122.017
47	142.673	136.170	139.209	120.407
48	144.038	135.265	140.879	120.932
49	144.860	136.732	137.442	120.477
50	145.879	132.630	137.891	119.497



**Table A1 (Continued)**

Time (min)	fEPSPs slope (% from baseline)			
	Theta-burst stimulation	Tetanic stimulation/control	Picrotoxin	Picrotoxin+CSD
51	144.940	133.761	141.229	119.307
52	146.429	134.679	139.499	119.601
53	143.795	134.537	140.074	120.376
54	143.910	134.489	141.011	120.252
55	145.888	136.187	141.681	120.213
56	143.798	134.613	140.682	119.807
57	143.459	134.847	138.466	120.165
58	145.765	133.266	141.027	120.644
59	143.657	135.394	140.110	120.631
60	142.599	137.055	138.713	120.501

**APPENDIX B**

## Statistical Values

The Statistical comparisons were performed by the analysis of variance test (one-way ANOVA). The  $\alpha$  level for statistical significance was set at  $P < 0.05$ .

### 1. One way ANOVA to compare the intensity of tetanic stimulation and theta-burst stimulation.

#### SUMMARY

<i>Groups</i>	<i>Count</i>	<i>Sum</i>	<i>Average</i>	<i>Variance</i>
Row 1	10	4.06	0.406	0.005671
Row 2	10	3.436	0.3436	0.009174

#### ANOVA

<i>Source of Variation</i>	<i>SS</i>	<i>df</i>	<i>MS</i>	<i>F</i>	<i>P-value</i>	<i>F crit</i>
Between Groups	0.019469	1	0.019469	2.622916	0.122718	4.413873
Within Groups	0.133606	18	0.007423			
Total	0.153075	19				

Since the P-value is  $0.122 > 0.05$ , hypothesis of equal intensity is not rejected.

### 2. One way ANOVA to compare the effectively induce LTP of tetanic stimulation and theta-burst stimulation.

#### SUMMARY

<i>Groups</i>	<i>Count</i>	<i>Sum</i>	<i>Average</i>	<i>Variance</i>
Column 1	10	1348.827	134.8827	1.216122
Column 2	10	1444.241	144.4241	1.569915

#### ANOVA

<i>Source of Variation</i>	<i>SS</i>	<i>df</i>	<i>MS</i>	<i>F</i>	<i>P-value</i>	<i>F crit</i>
Between Groups	455.1932	1	455.1932	326.7676	5.48E-13	4.413873
Within Groups	25.07433	18	1.393018			
Total	480.2676	19				

Since the P-value  $< 0.05$ , hypothesis of equal LTP induction is rejected.

**3. One way ANOVA to compare the amount of LTP in control group, picrotoxin group and CSD+picrotoxin group.**

SUMMARY

<i>Groups</i>	<i>Count</i>	<i>Sum</i>	<i>Average</i>	<i>Variance</i>
133.3496393	10	1343.563	134.3563	0.708622
137.8914343	10	1402.492	140.2492	1.170139
119.4970755	10	1201.496	120.1496	0.199205

ANOVA

<i>Source of Variation</i>	<i>SS</i>	<i>df</i>	<i>MS</i>	<i>F</i>	<i>P-value</i>	<i>F crit</i>
Between Groups	2135.168833	2	1067.584	1541.292	1.49E-28	3.354131
Within Groups	18.70169435	27	0.692655			
Total	2153.870528	29				

Since the P-value <0.05, hypothesis of equal LTP is rejected.

**4. One way ANOVA to compare the amount of LTP in theta-burst stimulation group, tetanic stimulation/control group, picrotoxin group and CSD+picrotoxin group.**

SUMMARY

<i>Groups</i>	<i>Count</i>	<i>Sum</i>	<i>Average</i>	<i>Variance</i>
Column 1	10	1343.563	134.3563	0.708622
Column 2	10	1402.492	140.2492	1.170139
Column 3	10	1201.496	120.1496	0.199205
Column 4	10	1444.241	144.4241	1.569915

ANOVA

<i>Source of Variation</i>	<i>SS</i>	<i>df</i>	<i>MS</i>	<i>F</i>	<i>P-value</i>	<i>F crit</i>
Between Groups	3371.488	3	1123.829	1232.309	2.53E-36	2.866266
Within Groups	32.83093	36	0.91197			
Total	3404.319	39				

Since the P-value <0.05, hypothesis of equal LTP is rejected.

## BIOGRAPHY

**NAME** Mr. Teerapol Saleewong

**BIRTHDAY** January 4, 1978

**PLACE OF BIRTH** Lampang, Thailand

### EDUCATION

- |           |  |
|-----------|--|
| 1996-1999 | B.S. (Mathematics), Chiang Mai University, Chiang Mai, Thailand.                                       |
| 2000-2001 | M.S. (Applied Mathematics), Chiang Mai University, Chiang Mai, Thailand.                               |
| 2006-2012 | Ph.D. Candidate in Biomedical Engineering, Faculty of Engineering, Chulalongkorn University, Thailand. |

**SCHOLARSHIP** University Development Commission Scholarship, U.D.C. (2000-2001).

### PRESENT APPOINTMENT

Lecturer in Mathematics, Department of Mathematics, Faculty of Science, King Mongkut's University of Technology Thonburi (KMUTT), Thailand.

### PUBLICATION

- [1] Saleewong, T., Srikiatkachorn, A., Maneepark, M., Chonwerayuth, A., Bongsebandhu-phubhakdi, S., *Computational approach to long-term potentiation in hippocampal CA1 area describes the efficacy of stimulation patterns*, ASIAN BIOMEDICINE (Accepted, 2012).
- [2] Saleewong, T., Srikiatkachorn, A., Maneepark, M., Chonwerayuth, A., Bongsebandhu-phubhakdi, S., *Quantifying altered long-term potentiation in the CA1 hippocampus*, JOURNAL OF INTEGRATIVE NEUROSCIENCE (Accepted, 2012).